

ALMA MATER STUDIORUM UNIVERSITA DI BOLOGNA

DOTTORATO DI RICERCA IN INGEGNERIA
ENERGETICA,NUCLEARE E DEL CONTROLLO AMBIENTALE

Ciclo XXV

Settore Concorsuale di afferenza:09/C2

Settore Scientifico disciplinare:ING-IND/10

TITOLO TESI

Numerical optimization,modeling and system evaluation of a
thermophotovoltaic hybrid panel

Matteo Greppi

Coordinatore Dottorato:
Prof. Antonio Barletta

Relatore:
Prof. Giampietro Fabbri

Esame finale Anno 2013

*Dedicato ai nonni
Giorgio,
Mariuccia,
Giulio.*

Abstract

Photovoltaic (PV) solar panels generally produce electricity in the 6% to 16% efficiency range, the rest being dissipated in thermal losses. To recover this amount, hybrid photovoltaic thermal systems (PVT) have been devised. These are devices that simultaneously convert solar energy into electricity and heat. It is thus interesting to study the PVT system globally from different point of views in order to evaluate advantages and disadvantages of this technology and its possible uses. In particular in Chapter II, the development of the PVT absorber numerical optimization by a genetic algorithm has been carried out analyzing different internal channel profiles (from 1st to 4th order) in order to find a right compromise between performance and technical and economical feasibility. Therefore in Chapter III, thanks to a mobile structure built into the university lab, it has been compared experimentally electrical and thermal output power from PVT panels with separated photovoltaic and solar thermal productions. Collecting a lot of experimental data based on different seasonal conditions (ambient temperature, irradiation, wind...), boundary collector inlet and outlet temperature and fluid velocity values, the aim of this mobile structure has been to evaluate average both thermal and electrical increasing and decreasing efficiency values obtained respect to separate productions through the year. In Chapter IV, new PVT and solar thermal equation based models in steady state conditions have been developed by software Dymola that uses Modelica language. This permits ,in a simplified way respect to previous system modelling softwares, to model and evaluate different concepts about PVT panel regarding its structure before prototyping and measuring it. The simplification about the model don't affect the accuracy of the results compared to previous more complicated ones and experimental data collected. Chapter V concerns instead the definition of PVT boundary conditions into a HVAC system. This was made trough year simulations by software Polysun in order to finally assess the best solar assisted integrated structure thanks to F_{save} (solar saving energy)factor. Finally, Chapter VI presents the conclusion and the perspectives of this PhD work.

Contents

1	Introduction	1
2	Optimization of a PVT panel/heat sink system using genetic algorithms	5
2.1	The mathematical model	6
2.2	Geometry optimization	9
2.3	Results	10
2.4	Conclusions	16
3	Experimental outdoor evaluation of the PVT panel efficiency	17
3.1	Experimental apparatus	17
3.2	Performance analysis	20
3.3	Results	21
3.4	Conclusion	29
4	Equation based modelling of PVT/ST panels	31
4.1	Introduction	31
4.1.1	Dangers of simulation	32
4.1.2	Model validation	32
4.2	Previous Excel collector model	33
4.3	Modelica Intro	33
4.4	Why Dymola?	34
4.5	Our Modelica/Dymola Model	34
4.6	Differences between Solar thermal and PVT model	37
4.7	Difference between Modelica and Excel Model	38
5	Boundary conditions for the PVT system analysis	41
5.1	Description of this work package	41
5.1.1	Solar Heating System Performance	41
5.1.2	Collectors Evaluated	43
5.1.3	Systems evaluated	45

5.2	System Analysis	50
5.2.1	Flow through DHW pre-heat system (DHW)	51
5.2.2	Auxiliary Heated Combi System	60
5.2.3	Large solar fraction system (SF-House)	70
5.2.4	Solar and Heat Pump (Solar+HP)	72
5.2.5	Solar Heat pump (integrated)	75
6	Conclusions	77
A	Fluid and Materials:	
	Temperature dependance	83
	Acknowledgements	87
	Bibliography	88

*A model must be wrong, in some respects, else it would be the thing itself.
The trick is to see where it is right*

Henry Bent

Chapter 1

Introduction

Photovoltaic solar panels generally produce electricity in the 6% to 16% efficiency range, while most of the incident radiation is lost to the environment as thermal energy, whereas, in comparison, a solar thermal collector can operate in the 60% to 82 ÷ 83% efficiency range. A lot of work has been done in the past to improve efficiency of PV panels, to reduce manufacturing costs and to integrate PV panels into walls and roofs of buildings. On the contrary, few efforts have been devoted in the past decades to the recovery of the dissipated thermal energy. Hybrid photovoltaic/thermal (PV/T) air-water collectors are devices that simultaneously convert solar energy into electricity and heat. The aim of these components is to increase the heat collected from cooling of a PV module so as to obtain two different energy outputs through one device. A PVT collector typically consists of a PV module on the back of which an absorber plate (a heat extraction device) is attached. Firstly, cooling the PV module we improve its electrical performance (electrical efficiency losses amount to 0.4% for each degree of increase of cell temperature with reference to standard test conditions (STC) $T_{amb} = 25^{\circ}\text{C}$ and $q'' = 1000 \text{ W/m}^2$) and secondly we collect the thermal energy produced, which would have otherwise been lost as heat to the environment. As reported by [1] the thermal performance of PV/T collectors is a bit lower than that of conventional thermal collectors due to worse absorbing surface. The principal advantages of this approach are: high combined efficiency in limited space (up to 40% savings in space with the same amount of energy produced), simultaneous cover of both electricity and thermal demands and possible use of thermal energy output for HVAC systems depending on the season. To raise the energy efficiency, many researchers have focused their attention on the development of hybrid PVT systems. The first hybrid air collectors were employed in a roof integrated structure in the Solar One house of the University of Delaware [2]. In a further development hybrid collectors were used

in the Solar Knoll residence at the same institute,[3], employing water as coolant. Comparison of both systems indicated a number of advantages and disadvantages between the two fluids: water is a more efficient transport fluid with higher heat conductivity and high thermal capacity; on the other hand using of water requires more extensive modifications to enable water tight piping and fittings and corrosion-free construction. Air based PVT collectors are preferred to water ones due to their low cost and lower material usage. However, heat extraction by air circulation is limited because of the low density, small volumetric heat capacity and small thermal conductivity of air . Recently [4] have studied four possible PVT collector configurations: unglazed with tedlar (tedlar is called a PVF polyvinyl fluoride film) (UGT), glazed with tedlar (GT), unglazed without tedlar (UGWT) and glazed without tedlar (GWT). It was found that the daily efficiency of the system with water is higher than with air except for glazed without tedlar . Based on an exergy and cost analysis, [5] analyze some of the parameters affecting PV/T performance (both electrical and thermal) such as covered versus uncovered PV/T collectors, optimum mass flow rate, absorber plate parameters (i.e. tube spacing, tube diameter, fin thickness), absorber to fluid thermal conductance and configuration design types. Water PVT glazed flat plate collector system results the most promising to develop . Also [6] conducted an experimental and numerical validation to determine the suitability of using a glazed or unglazed PVT system from the thermodynamical viewpoint. In their experiment, six different parameters were considered and evaluated for both glazed and unglazed conditions (PV cell efficiency, packing factor, water mass to collector area ratio, wind velocity, solar radiation and ambient temperature). They have found that the glazed system gives better results when viewed from the energetic point of view if the aim is to maximize the quantity of either the thermal or the overall energy output, whereas from the exergy analysis, the unglazed collector gives better results. Increase in the PV cell efficiency, packing factor, water mass to collector area ratio and wind velocity gives better results for an unglazed system, whereas the increase in on-site solar radiation and ambient temperature is favourable for the glazed system. [7] have grouped the design concepts of water-type PVT collectors into four main types: sheet-in-tube collectors, channel collectors, free flow collectors and two absorbers collectors. From the point of view of overall performance and structural simplicity, the single low emission glazing sheet-in-tube PVT collector is regarded as the most promising design.[16] have done a detailed analysis of the energy yield of systems with covered sheet and tube PVT collectors. Concerning annual PVT systems efficiencies working at very high fluid temperatures(tap water heating) ,they found a little lower electrical efficiency(−14%)compared to PV panel and a

lower (−19%) thermal efficiency due to high absorber emissivity and the withdrawal of electrical energy. PVT collectors can be further upgraded as is the case in BIPVT (building integrated thermal photovoltaic collectors), which can be used in buildings (see [14]). More recently [18] have proposed, after fixing the most appropriate concept configuration, an efficient single glazed PVT panel with a thermal efficiency at zero reduced temperature equal to 79%. Then [17] have analysed the prototype experimentally indoor by means of a sun simulator and numerically by Transys simulations obtaining that the use of efficient PVT collectors can be more advantageous than standard PV and solar thermal components, not only from an energetic point of view, but also considering the exergy and the primary energy saving.

Chapter 2

Optimization of a PVT panel/heat sink system using genetic algorithms

Focusing on PVT technology double outputs, it seemed interesting, for the first part of our work, to focus on optimization of the thermal efficiency of the PV/T system absorber concerning the reference internal upper and lower channel profile of an industrial heat sink (see[22]). To study this problem, a mathematical model for the heat sink is used which is able to analyze the thermal and fluid dynamical alterations induced by changes in the channel profile. To optimize the performance of the absorber heat sink in terms of heat transfer to the fluid, a genetic algorithm is employed to maximize the equivalent Nusselt number Nu_e and compared effectiveness E_c under pressure and maximum material constraints. The velocity and temperature distributions in the channels cross section under conditions of uniform, imposed heat flux at one wall ($1000 W/m^2$), periodicity at two walls and insulation at the other are computed with the help of a finite element model (a global heat transfer coefficient is calculated). [19] already proposed previously a genetic algorithm for thermal efficiency optimization of a heat sink analyzing different profiles for its fin (asymmetrical and symmetrical longitudinal wavy fins) and then in 2009 [20] a multi-objective genetic optimization of the heat transfer from longitudinal wavy fins.

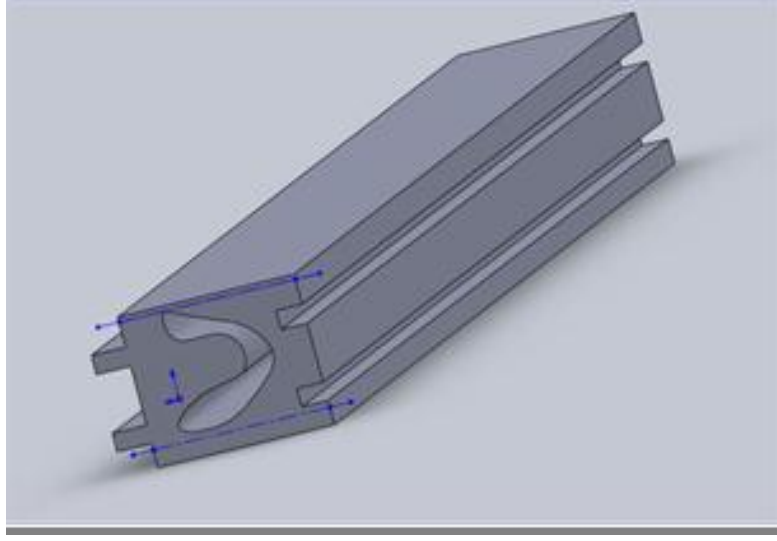


Figure 2.1: geometry of the heat sink characteristic module

2.1 The mathematical model

Let us consider a modular heat sink composed of a large number of identical ducts where a coolant fluid flows in laminar regime under the same conditions, as shown in (2.1). A heat flux q'' is uniformly imposed on one surface of the heat sink, while the opposite is thermally insulated.

The inner surface of the ducts is divided into four stretches, each corresponding to one side of the perimeter of its cross section. Of these, two are kept straight and two (the side walls) can vary their shape according to a polynomial law. Externally, it is delimited by two flat surfaces and two sides having matching shapes which allow two adjacent ducts to be assembled together. In particular, on one side two trapezoidal protrusions are located, while on the opposite side are two trapezoidal cavities. In general, the duct wall must be sufficiently thick to ensure the mechanical consistence of the heat sink. Moreover, on the side where the heat flux is imposed, it must be sufficiently thick to allow screws to be inserted to assemble the heat sink to the system to be cooled. Therefore, some limits must be imposed to the wall thickness on the four sides of the duct in our reference prototype(2.2).

Let us choose an orthogonal coordinate system, where the x axis is laid along the coolant flow direction and the y axis is orthogonal to the surface where the heat flux is imposed. Moreover, let a be the internal duct height in the y direction, b the thickness of the wall where the screws are inserted, d the external duct height, e the external duct width, $f_1(y)$ and $f_2(y)$ arbitraries functions which describe the profiles of the two wavy internal surfaces of the

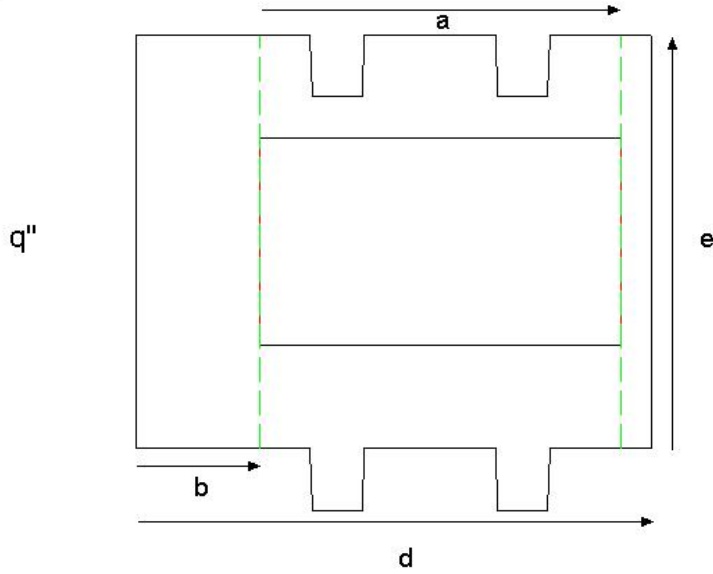


Figure 2.2: reference prototype of the heat sink

duct, and Ω_1 and Ω_2 the external contour line of the duct cross section on the side where fins and cavities are, respectively. Since the dynamic and thermal behavior of the whole heat sink is periodic in the z direction, the analysis can be limited to a single duct. The following hypotheses are now introduced:

- the system is at steady state;
- velocity and temperature profiles are fully developed;
- fluid and solid properties are uniform and temperature independent ;
- viscous dissipation within the fluid is negligible;
- natural convection is negligible in comparison to the forced convection;

Under such conditions the coolant flow is described by the momentum equation, 2.1:

$$\frac{\partial^2 u}{\partial y^2} + \frac{\partial^2 u}{\partial z^2} = 1/\mu \frac{\partial p}{\partial x} \quad (2.1)$$

where u is the fluid velocity, p the generalized pressure, which includes the gravitation potential, and μ the dynamic viscosity. 2.1 must be integrated by imposing, as a boundary condition, that the velocity is zero on the contact

surface between the fluid and the solid wall. In the fluid, the temperature T_c must satisfy the following energy balance equation 2.2:

$$\frac{\partial^2 T_c}{\partial y^2} + \frac{\partial^2 T_c}{\partial z^2} = \frac{\rho_f c_p}{k_c} u \frac{\partial T_c}{\partial x} \quad (2.2)$$

ρ_f , c_p and k_c being the fluid density, specific heat and thermal conductivity, respectively. In the finned plate, the temperature must instead satisfy the energy equation for a solid, 2.3:

$$\frac{\partial^2 T_f}{\partial y^2} + \frac{\partial^2 T_f}{\partial z^2} = 0 \quad (2.3)$$

where T_f is the temperature of the fin. 2.2 and 2.3 must be integrated by imposing boundary conditions corresponding to the following 2.4-2.5:

- the temperature and the heat flux in the normal direction at the interface between the solid and the fluid are identical;
- the heat flux in the normal direction is zero on the insulated flat surface and is equal to q'' on the opposite flat side of the duct.

$$T_f[y, \omega_1(y)] = T_f[y, \omega_2(y)] \quad (2.4)$$

$$[\partial T_f / \partial N]_{[y, \omega_1(y)]} = [\partial T_f / \partial N]_{[y, \omega_2(y)]} \quad (2.5)$$

where functions $\omega_1(y)$ and $\omega_2(y)$ provide the value of the z coordinate in ω_1 and ω_2 respectively, and N is normal to the two lines. It is also necessary to impose a temperature value in one point of the studied domain. Due to the complexity of the problem velocity and temperature distributions must be determined in a numerical way. The finite volume method described in [21] and [19] can also be conveniently applied to the investigated case. In these works parameters a, b, d, e and the profile functions $f_1(y)$ and $f_2(y)$ describe the geometry of the finned conduit. In the studied domain, z coordinate is equal to $f_1(y)$ on a lateral fin profile and to $2e - f_2(y)$ on the other. Dimensionless variables can be obtained by normalizing all geometrical parameters with d:

$$\alpha = a/d, \beta = b/d, \epsilon = e/d, \eta = y/d, \\ \varphi_1(\eta) = f_1(\eta d/d), \varphi_2(\eta) = f_2(\eta d/d).$$

After determining the velocity and temperature distributions, bulk temperature, global heat transfer coefficient, the equivalent Nusselt number Nu_e , compared effectiveness E_c and normalized hydraulic resistance can be defined and calculated as in [21] and [19]. In particular, the equivalent Nusselt number, 2.6, is defined as the Nusselt number which would be obtained if the same heat flux removed by the modular heat sink were dissipated in a flat wall channel of the same height:

$$Nu_e = \frac{h2d}{K_c} \quad (2.6)$$

$$\epsilon = \left(\frac{-dp/dx}{w_t/2e} \right) \left(\frac{12\mu}{d^3} \right) \quad (2.7)$$

$$E_c = \frac{q''}{q_r''} \quad (2.8)$$

The compared effectiveness is defined as the ratio between the heat flux removed by the modular dissipator and that dissipated in a flat wall channel with the same hydraulic resistance 2.8, and the normalized hydraulic resistance 2.7 is the ratio between the hydraulic resistance of the modular dissipator and that of a flat wall channel of the same height.

2.2 Geometry optimization

To optimize the geometry of the duct in order to maximize the equivalent Nusselt number and the compared effectiveness, a genetic algorithm has been used. A polynomial form has been assigned to the functions $f_1(y)$ and $f_2(y)$. These functions have then been represented by $n_1 + 1$ and $n_2 + 1$ parameters, consisting of the values of the functions in $n_1 + 1$ and $n_2 + 1$ equidistant points in the domain, n_1 and n_2 being the polynomial orders. Besides the Rp_{max} limits the condition of constrained finned plate volume has been taken into account imposing the average thickness σ_s . Moreover by imposing, for example, limits on the values of the derivatives of $f_1(y)$ and $f_2(y)$ at the end points (corresponding to constraints on the profiles curvature), the number of possible finned tube geometries can be reduced. After fixing the order of the polynomial function which describes the fin profile (from 1st to 4th order) a new profile is chosen as a prototype(2.6). The prototype is then reproduced with random mutations uniformly distributed between -10 and +10, in order to compose an initial population of 10 samples (including the prototype). For each sample the compared effectiveness is computed. The two samples with the best rank are selected and reproduced with the mutation rule described

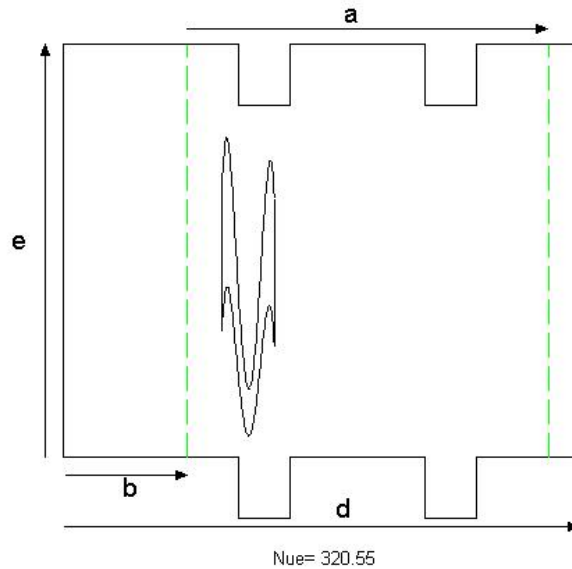


Figure 2.3: unconstrained module

above. The new generation is evaluated, selected and reproduced in the same way. The process continues until there is no significant improvement in the compared effectiveness of the best sample or is reached a set number of simulations. The population dimension is chosen on the basis of the polynomial order. With low orders very numerous populations are not required to keep the algorithm from stopping in correspondence of a local maximum whereas larger populations are required for higher order profile functions. In the algorithm it is also possible to impose a local fin thickness (an upper and a lower limit to the fin profile by rescaling the parameter before evaluating the performances).

2.3 Results

Several tests using the GA have been carried out in order to find the geometries of the channel which maximize the Nusselt number Nu_e and E_c (compared effectiveness). We start from the unconstrained industrial module heat sink (2.3):

The module fitness rapidly increases with the channel squeezing towards the heated side but industrial manufacturing by extrusion would not be possible and R_p becomes too high.

Now we show (2.4-2.5) the best profile functions in terms of equivalent Nusselt number with second, third or fourth polynomial order with bonds

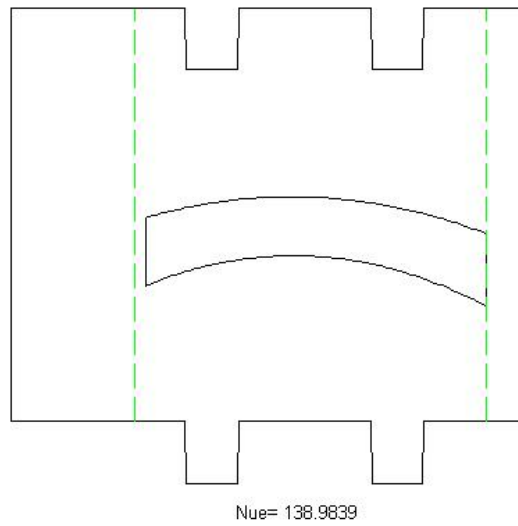


Figure 2.4: 2nd order prototype $\sigma_s/d = 0.9R_p$ unconstrained

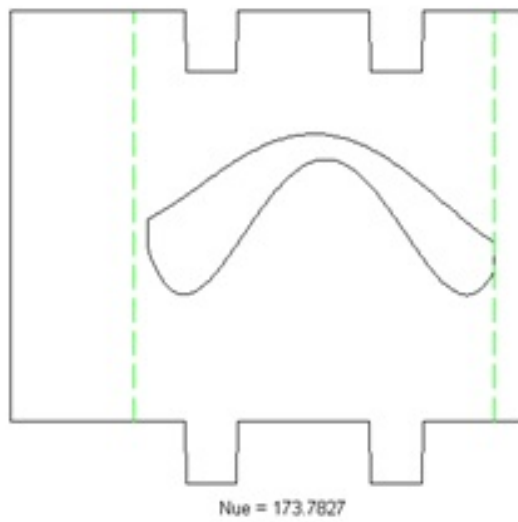


Figure 2.5: 4th order prototype $\sigma_s/d = 0.9R_p$ unconstrained

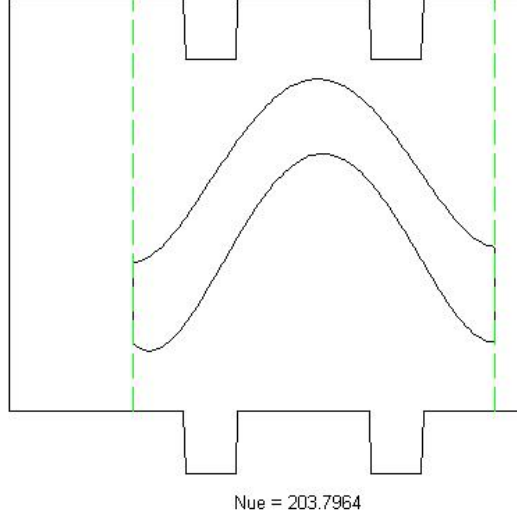


Figure 2.6: 4th order prototype $\sigma_s/d = 0.85$ $2000R_{ps}$

only on σ_s/d (fixed volume). Now for a more realistic analysis a constraint was imposed on R_p , namely 50, 100, 500, 1000, 2000 times the standard normalized reference value of a rectangular channel, 2.9:

$$R_{ps} = \frac{6\mu}{d^3}e. \quad (2.9)$$

which corresponds to the starting geometry. This has the consequence of decreasing the maximum cold plate efficiency. Stagnation occurs at the corners, which dampens the convective effect(2.6-2.7-2.8-2.9-2.10). Lowering the maximum limit of the hydraulic resistance down 10 R_{ps} we note that algorithm cannot operate for physical limits of the problem searching optimal thermal solutions. (2.11) shows how σ_s/d ratio for different constraints and 4th polynomial order influence module fitness. Accepting for our profile high hydraulic resistance value up to 2000 R_{ps} , we can observe a monotonous curve until the σ_s/d ratio is equal to 0.85.

After this value pressure losses are too high as the energy cost to pump the water inside the heat sink. With a different objective (maximize heat sink channel profile fitness with low pressure loss) lower σ_s/d ratio near 0.7 gives good result in terms of dissipating efficiency.

Now we show the ratio between compared efficiency E_c as a function of the hydraulic resistance of the channel for the 4th order profiles evaluated (2.12).

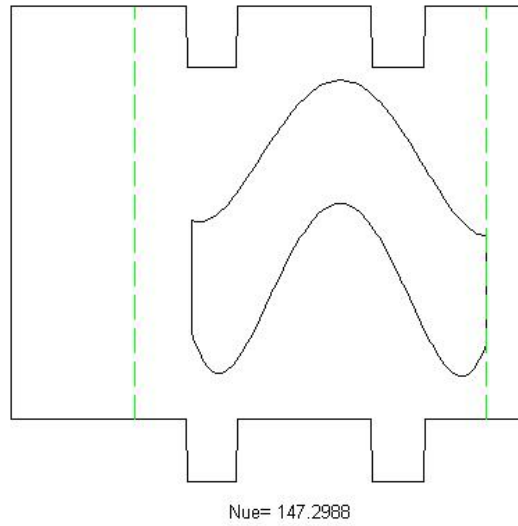


Figure 2.7: 4th order prototype $\sigma_s/d = 0.85$ $1000R_{ps}$

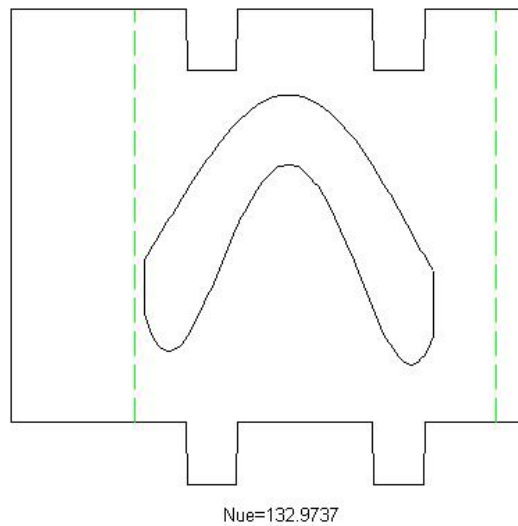


Figure 2.8: 4th order prototype $\sigma_s/d = 0.8$ $500R_{ps}$

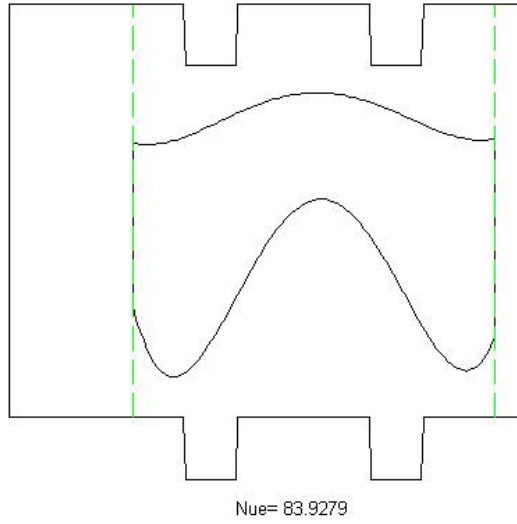


Figure 2.9: 4th order prototype $\sigma_s/d = 0.7 \ 100R_{ps}$

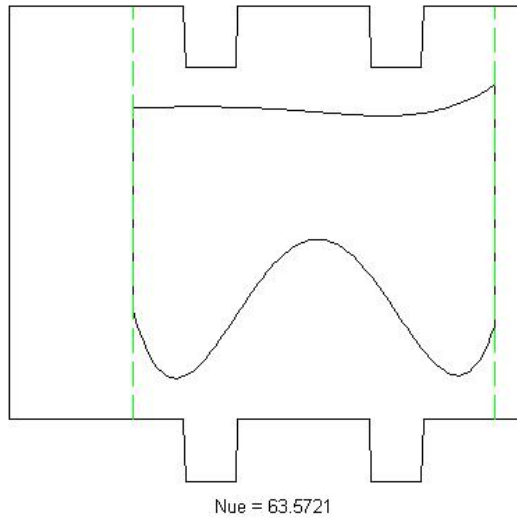


Figure 2.10: 4th order prototype $\sigma_s/d = 0.65 \ 50R_{ps}$

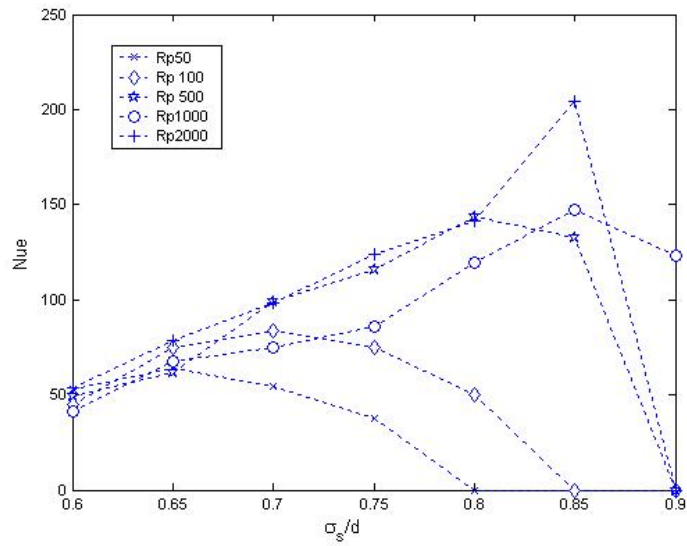


Figure 2.11: Nu_e as a function of σ_s/d for 4th order profiles

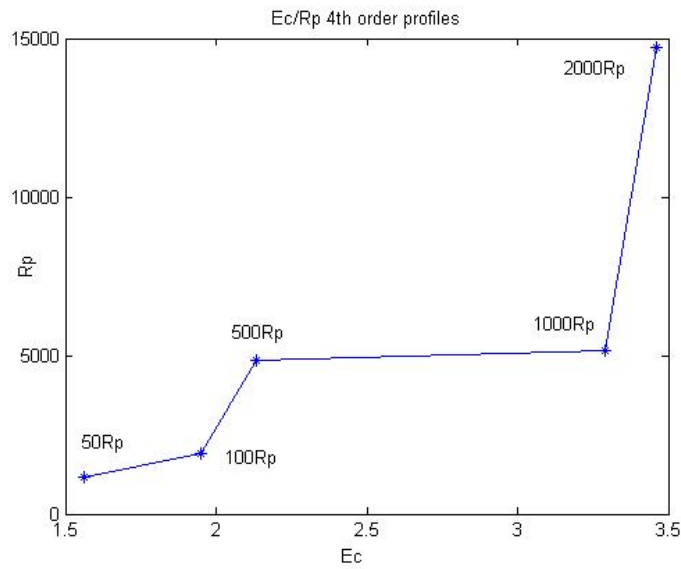


Figure 2.12: Correlation $E_c - R_p$ 4th order profiles

It is interesting to underline that is not so linear the graph with the dependent variable, but for a particular value of R_p , E_c remains almost constant and then returns to increase (effect of profile's local convective thermal exchange).

2.4 Conclusions

From the results showed in this chapter, it's evident the efficiency improving of our heat sink due to upper and lower reference internal channel profile modifications from 2nd to 4th order. For a realistic analysis we have, anyway, to reach an optimum compromise for our profile taking account to constraints as fixed volume, hydraulic resistance and profiles local convective thermal exchange in order to obtain the best working solution that has to be technically and then economically feasible. For this reason we can't choose the profile that stretches our channel area section in order only to maximize thermal exchange area between absorber and fluid but a less performing well optimized and simpler one that will be anyway more efficient for the specific thermal package respect to the standard channel profile.

Chapter 3

Experimental outdoor evaluation of the PVT panel efficiency

In this section the aim has been instead to study the PVT system experimentally outdoor to assess the increase in performance for a particular Italian north-east location(Forli) as part of a closed loop single phase water CDU (coolant distribution unit) in laminar forced convection. The daily tests have been done in this work in comparison with a PV (photovoltaic) and a ST (solar thermal) system: this taken on the experimental rig shows an increasing electrical production up to $+15 \div 20\%$ with a little decrease of thermal efficiency ($-10 \div 15\%$). These results are obtained for particular climatic conditions and operating collector temperatures by a single glazed hybrid PVT water panel.

3.1 Experimental apparatus

Concerning the description of the test rig.(3.1), three different type of panels (PV, Solar Thermal, PVT) have been built : a PV cells glazed panel ; a hybrid PVT glazed collector, consisting of the PV cells (with anti-reflective coating) glued for a good thermal contact on the cold off-the-shelf plate that works as thermal absorber all enclosed into an insulating frame of polyurethane foam; a solar thermal collector, consisting of a frame with polyurethane foam and a cold plate of the same design as that used for the PVT collector which acts as the black absorber plate ($\alpha = 0.92$). A static air layer separates glass cover from absorber surface (PV cells or black absorber) for each panels. The collector square active area is 0.36 m^2 . For PV and PVT modules,

monocrystalline $125 \times 125 \text{mm} \pm 1.0 \text{ mm}$ PV cells are soldered to silver ribbon strings that connect them in series. For PVT one the cells, thanks to a thermally conductive silicon paste, are laid over the absorber in order to ensure a satisfactory thermal contact between the heat sink and the solar cell panel. Ribbon cavities of the same depth as the thickness of the strings provide a satisfactory mechanical connection of the two elements. A junction box containing bypass diodes eliminates the hot spots due to the presence of cells partially shaded, whereas a battery charge controller prevents overcharging and overvoltage of the battery that accumulates electricity produced by the panels. The hydraulic circuit consist of a fluid flow circulator (with three different velocities that can be chosen), hoses of Rilsan, a thermostatic water bath, a flow meter measuring the flow rate to the hybrid and solar panel and a needle valve to adjust the hydraulic resistance of the solar panel and balance the different branches. As a coolant, water is employed as it is safer than glycol for lab testing. T-type thermocouples with a measurement range between -200°C to $+400^\circ\text{C}$ (with an uncertainty of $\pm 1^\circ\text{C}$ or $\pm 0.75\%$) provide temperature values. The global irradiation G incident on the inclined surface (33°) is obtained from the measurements of HT 204 pyranometer and also compared with ENEA tables for the location and optimum tilt angle (Forli, 33°). This device has a measurement range between 0 and $1999 \text{ W}/(\text{m}^2\text{C})$ with an uncertainty of $\pm 10 \text{ W}/\text{m}^2$. A commercial digital multimeter collects DC voltage values for open circuit mode and DC voltage and DC current values for maximum power point mode with an uncertainty of $\pm 0.5\%$ and $\pm 1\%$ respectively (these values are necessary for our panel comparisons). A dedicated Lab View interface has been created and programmed to easily collect and process the measured data. In our mobile test rig layout above described consisting of the three different panel structures (PV,ST,PVT) and shown in (3.2), the liquid exiting the plates is cooled in the thermostatic water bath and returned through pumping by a flow circulator to the cold plates inlet at a fixed temperature. The three values employed for volume flow rate are 0.018 , 0.03 and $0.0425 \text{ m}^3/\text{s}$. The T-type thermocouples are connected to a digital data acquisition interface, which also measures the frequency signals from circuit flow meters to determine the mass flow rate in the two separated loops. The HT 204 pyranometer with the sensor mounted complanar with the plane of the collector aperture is allowed to equilibrate for at least 10 minutes before data acquisition.

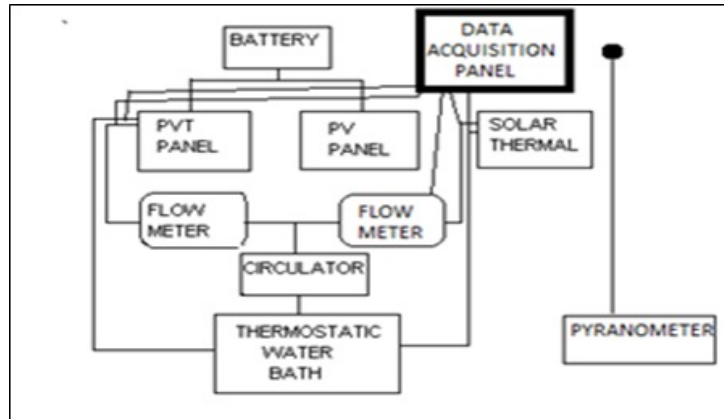


Figure 3.1: simplified apparatus scheme

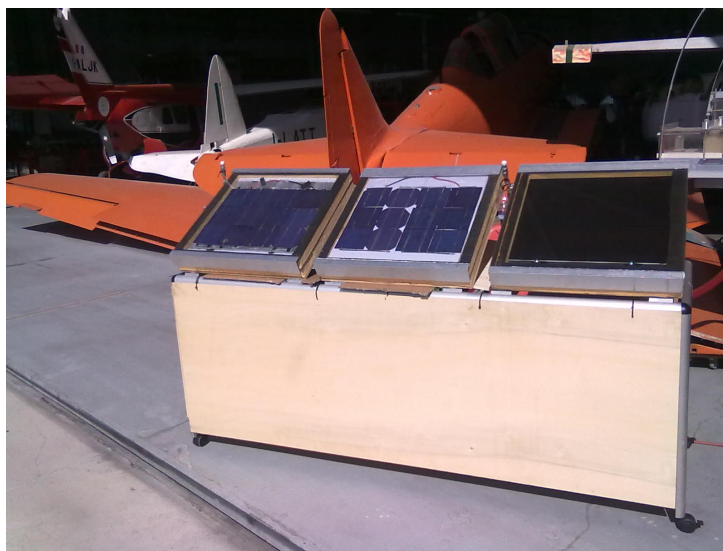


Figure 3.2: experimental apparatus scheme

3.2 Performance analysis

The instantaneous efficiency η_t of the solar collector absorber used for our analysis is calculated following [23] by the standardized equation obtained by Bliss(3.5) and reported in [24]and in [25], assuming that most of the radiation is nearly normal to the collector and U_d and F_r do not vary greatly in the range of operation of the collector. The heat removal factor F_r is the ratio between the actual useful energy gain of a collector and the useful gain if the whole collector were at the fluid inlet temperature, U_d the thermal losses coefficient of the panels through the edge, the bottom and the front, T_i the inlet fluid temperature, T_u the outlet fluid temperature and T_{abs} the absorber temperature, T_a the ambient temperature and G is the global irradiation incident on the inclined surface (33°) of the panel. This standardized equation is derived from an instantaneous energy balance at the absorber 3.1:

$$Q_u = A_c[G(\tau\alpha) - U_d(T_{abs} - T_a)] \quad (3.1)$$

and from the definition of thermal efficiency for the collector 3.2:

$$\eta_t = \frac{Q_u}{GA_c} \quad (3.2)$$

where Q_u is the useful heat output by the panels, τ and α transmittance and absorbance factors respectively and A_c the thermal absorber area. Considering that Q_u can also be expressed by means of 3.3:

$$Q_u = mc_p(T_u - T_i) \quad (3.3)$$

and substituting F_r value 3.4:

$$F_r = \frac{mc_p(T_u - T_i)}{A_cG(\tau\alpha) - U_d(T_i - T_a)} \quad (3.4)$$

we obtain the known formula of the Hottel- Whillier-Bliss equation 3.5:

$$\eta_t = F_r[(\tau\alpha) - U_d(T_i - T_a)/G] \quad (3.5)$$

Concerning the electrical calculations, for the first period of test we have measured, only for PV and PVT panels, open circuit voltage V_{oc} (which is the maximum voltage available from a solar cell, which occurs at zero current) and relative ΔV percentage differences. Maximizing V_{oc} is good for high conversion efficiencies. Silicon solar cells on high quality single crystalline material have open-circuit voltages of up to 700 mV under global and direct normal Air Mass 1.5 spectra (reference to report PV cell measurements).

The multicrystalline silicon devices on PVT panel working near this low operating temperature ($25^{\circ}C$) show higher open-circuit voltages compared with PV panel operating values (due to the latter's higher absorber temperature). Concerning the electric load, efficiency is given by the following 3.6:

$$\eta_{es} = \frac{I_m V_m}{GA_c} \quad (3.6)$$

The reliability of PV module performance on the temperature is given by 3.7:

$$\eta_e = \eta_{es}(1 - \beta(T - 25^{\circ}C)) \quad (3.7)$$

where β is the temperature cell coefficient, that defines how much your panel's power output decrease as the temperature rises.

For the second period of our tests, the difference between V_{oc} and V_{cc} PVT and PV values (load influence) and its influence on PVT thermal efficiency are shown from Table 3.1 and Table 3.2.

3.3 Results

The measurement campaign began on September 2011 and lasted till the end of October 2011, subsequently it was started again at the beginning of July 2012 and was concluded at the end of the same month, with a final period of measurements in September 2012 in order to cover satisfactorily two different outdoor seasonal conditions (Summer and Autumn). The structure was located in a university lab in Forlì, in the North East of Italy, close to the Adriatic Sea. The main goal of the analysis was initially to measure instantaneous thermal efficiency η_t , increasing or decreasing percentage ΔT_{in-out} (difference between inlet and outlet collector temperatures from ST and PVT panels), open circuit voltage V_{oc} and ΔV_{oc} (difference between tension DC values from PV and PVT panels). These values have been measured to compare ST, PVT and PV outputs under the same outdoor operating conditions. The second period of the tests was also focused on the measure of the differences between V_{oc} and V_{cc} voltages so as to assess also which is the effect of photo-conversion on PVT thermal efficiency. Closed electric circuit results are based on a 3Ω resistance, this value being the one chosen for our tests. Below are described only some of the most significant clear sunny days of tests with negligible influence of the wind. Testing thermal collector efficiency according to [23], a linear Least Squares (LS) fitting proves sufficient to describe the experimental data with a global efficiency measure uncertainty of less than 6%.

Day1.(29/9/2011): A typical sunny summer afternoon. The ΔT_{in-out} percentage difference between ST and PVT panels starts from 7% at 15:45. Instead the increase of ΔV_{oc} between PV and PVT panels starts from +26% due to hot PV cell operating temperature. With the decrease of T_a and irradiation, it is evident ΔT_{in-out} percentage continuous increasing due to the higher influence of worse PVT absorbing surface on less available thermal energy and the decrease of ΔV_{oc} till 12% principally due to PV panel slow cooling.

Day2.(11/10/2011): Autumn afternoon with T_a near 25°C. ΔT_{in-out} percentage decrease is closed to 16 ÷ 17% instead ΔV_{oc} increase has reached +22 ÷ 23% due to high cell operating temperature.

Day3.(12/10/2011): Autumn morning with T_a around 22 ÷ 23°C, ΔT_{in-out} percentage decrease near 20% due to low ambient temperature and ΔV_{oc} closed to 26% (cell temperature is high yet).

Day4.(18/10/2011): Typical cool autumn morning with T_a near to 15°C. In central hours it is outstanding ΔT_{in-out} percentage decrease near to 32 ÷ 33% while in sunny September days has not reached 15%. ΔV_{oc} is fixed to +18 ÷ 20% far from 30% increase of typical sunny days.

Day5.(12/7/2012): The last day shown regards last summer(2012) measures where we compare also PV and PVT results on power point mode with the closed circuit resistance equal to 3 Ω (arbitrary chosen for our tests). Besides decreasing electric outputs, on the specific thermal efficiency graph it is clear the translated efficiency curve from ST to PVT thermal and power point mode due to both worse PVT absorbing properties and PV cell efficiency.

The results of measures carried out from the early morning in summer to late afternoon in autumn regarding two different measuring years (2011 and 2012) show a marked advantage gained through the use of PVT panels in terms of an increase of ΔV_{oc} up to a central hour peak of 30% in hot summer days with respect to PV panel. This at the expense of a decrease percentage ΔT_{in-out} respect to solar thermal panel by 10 ÷ 15%. Typical autumn days show instead a thermal average decrease of 30% with an increasing of ΔV percentage that reaches a peak of +20%. These carried out a medium annual increasing electric production up to +15 ÷ 20% with a little decrease of thermal efficiency (-10 ÷ 15%). The influence of the thermal modules inlet temperature, under the outdoor conditions involved, is to cause a slight decrease in thermal performance going from 15°C to 18-20°C (-2%). Concerning fluid flow three mass flow rates from 0.03 to 0.0425 m³/s (1.85 to 2.55 l/min) were analyzed for all daily tests. Decreasing mass flow rate there is a little increase ability to remove heat from the panel although not relevant in terms of efficiency for the values analyzed.

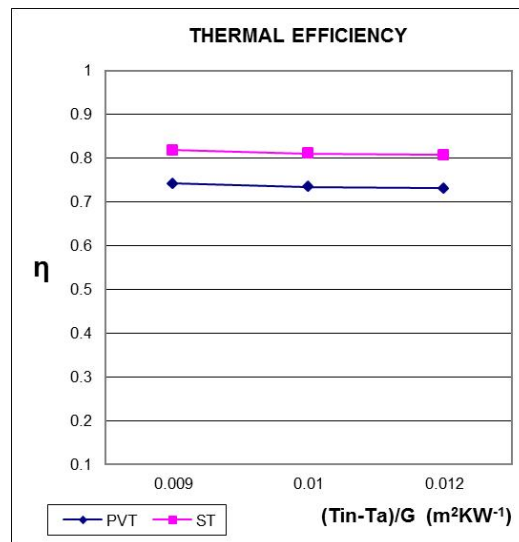


Figure 3.3: September 29th 2011 PVT SINGLE GLAZED 0.018 m³/s

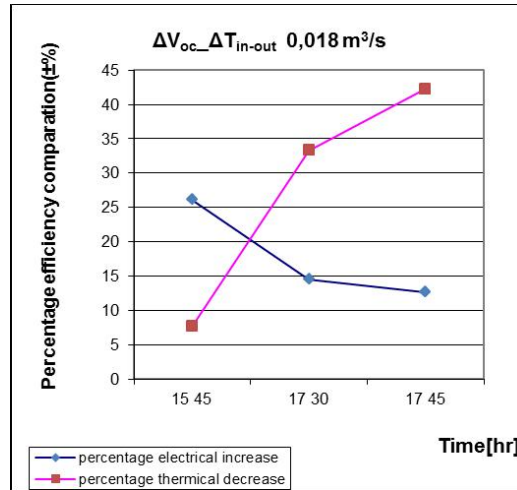


Figure 3.4: September 29th2011 PVT SINGLE GLAZED 0.018 m³/s

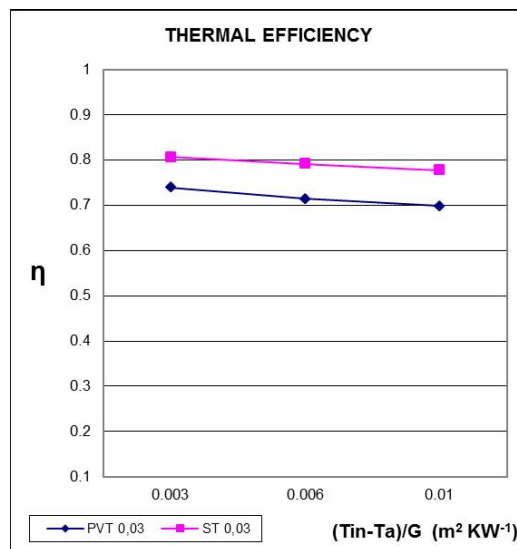


Figure 3.5: October 11th2011 PVT SINGLE GLAZED 0.03/0.0425 m³/s

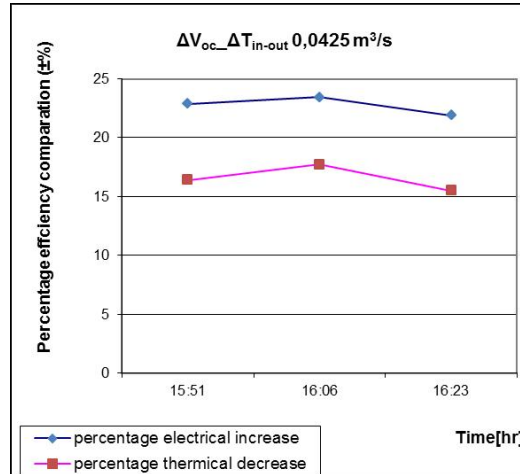


Figure 3.6: October 11th 2011 PVT SINGLE GLAZED 0.03/0.0425 m³/s

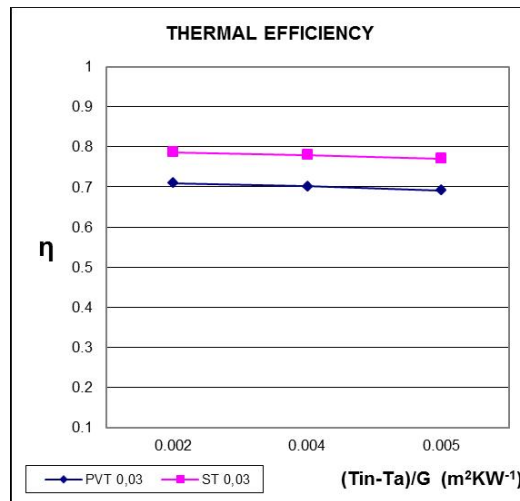


Figure 3.7: October 12th 2011 PVT SINGLE GLAZED 0.03 m³/s

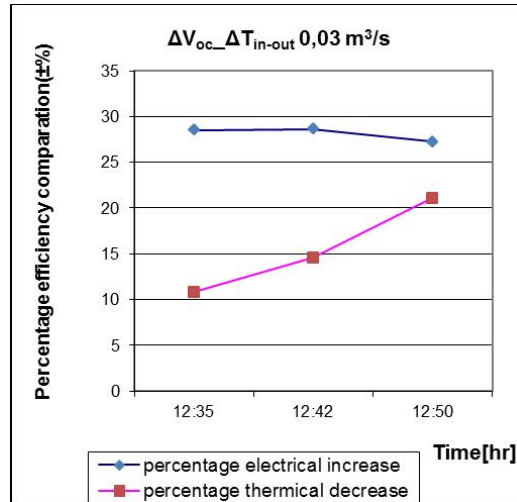


Figure 3.8: October 12th 2011 PVT SINGLE GLAZED 0.03 m³/s

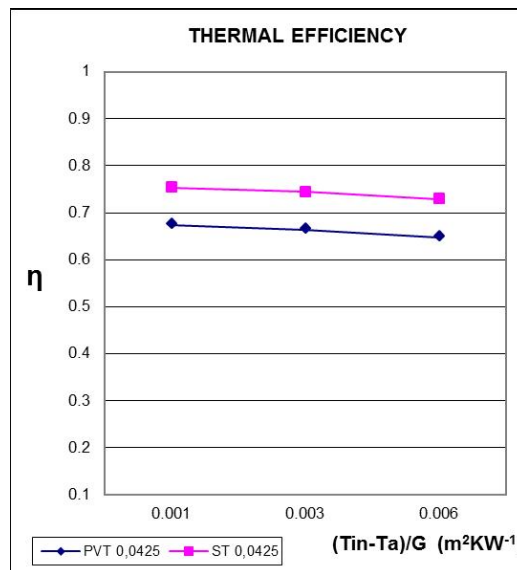


Figure 3.9: October 18th PVT SINGLE GLAZED 0.0425 m³/s

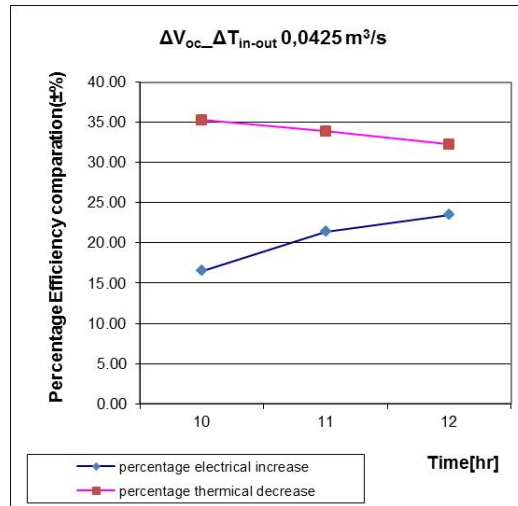


Figure 3.10: October 18th 2011 PVT SINGLE GLAZED 0.0425 m³/s

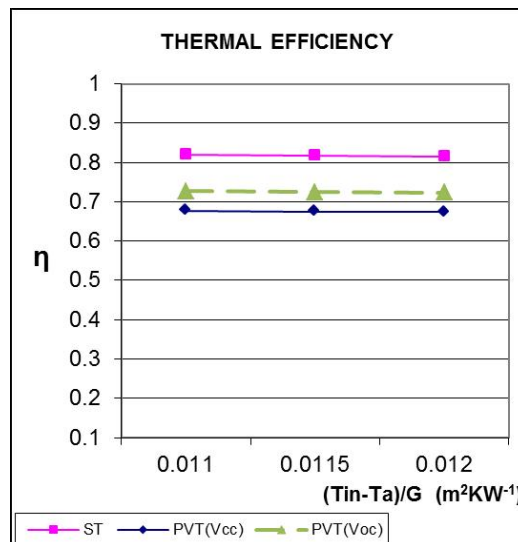


Figure 3.11: Thermal efficiency comparison (July 12th 2012)

	PVT(V_{oc})	PV(V_{oc})	$\Delta V(\%)$	Hour
29/09/2011(A)	6.75	5.35	26.2	15:30
29/09/2011(A)	6.56	5.82	12.7	17:45
11/10/2011(A)	6.86	5.70	20.4	17:00
11/10/2011(A)	6.62	5.90	12.2	17:45
12/10/2011(M)	6.85	5.33	28.5	11:45
12/10/2011(M)	6.77	5.32	27.3	12:45
17/10/2011(A)	6.97	5.78	20.6	15:37
17/10/2011(A)	6.83	5.95	14.8	16:30
18/10/2011(M)	6.97	5.98	16.6	10:00
18/10/2011(M)	6.90	5.69	21.3	11:00
18/10/2011(M)	6.83	5.53	23.5	12:00

Table 3.1: ΔV_{oc} PVT/PV comparison

	PVT(V_{oc})	PVT(V_m)	$\Delta V(\%)_{PVT}$	PV(V_{oc})	PV(V_m)	$\Delta V(\%)_{PV}$	$\Delta V(\%)_{PVT-PV}$
12/07/2012(M)	6.93	6.40	8.3	5.82	5.20	11.9	23.1
12/07/2012(A)	6.90	6.30	9.5	5.93	5.40	9.8	16.7
13/07/2012(M)	6.87	6.37	7.8	5.82	5.30	9.8	20.2
13/07/2012(M)	6.86	6.30	8.9	5.66	5.10	9.0	23.5
16/07/2012(A)	6.87	6.30	9.0	5.69	5.05	10.7	24.8
17/07/2012(M)	6.85	6.30	8.7	5.55	4.99	11.2	26.3
17/07/2012(A)	6.81	6.20	9.8	5.42	4.94	9.7	25.5
18/07/2012(M)	6.82	6.20	10.0	5.48	4.95	10.7	25.3
18/07/2012(A)	6.81	6.29	8.3	5.30	4.83	9.7	30.2
19/07/2012(M)	6.85	6.17	11.0	5.78	5.20	11.2	18.7
19/07/2012(A)	6.90	6.39	8.0	5.68	5.20	9.2	22.9
20/07/2012(M)	6.88	6.34	8.5	5.58	5.05	10.5	25.5
20/07/2012(M)	6.88	6.36	8.2	5.60	5.05	10.9	25.9
25/07/2012(A)	6.87	6.32	8.7	5.50	5.00	10.0	26.4
26/07/2012(M)	6.86	6.26	9.6	5.70	5.14	10.9	21.8
26/07/2012(A)	6.88	6.32	8.9	5.42	4.93	9.9	28.2
27/07/2012(M)	6.83	6.30	8.4	5.44	5.00	8.8	26.0
27/07/2012(A)	6.82	6.19	10.2	5.47	5.00	9.4	23.8
25/09/2012(A)	6.90	6.12	12.7	5.66	5.00	13.2	22.4

Table 3.2: Comparison of voltages for PVT and PV mod

3.4 Conclusion

In order to analyze results for the specific seasonal conditions and the operating collector temperature studied the electrical output is considered first. It is noticeable that the average annual efficiency gain due to cell cooling is rather high (15-20%). In fact hot cell temperature reaches 60°C in the hottest hours of the day, very far from standard project ambient temperature (25°C). Also in middle seasons, despite a lower thermal exchange, cells temperatures are always higher than 25°C thus a positive efficiency gain is always obtained. From the thermal point of view the average annual efficiency is 10 ÷ 15% less than for the solar thermal collector. Analyzing the thermal efficiency graph, the PVT power point mode curve shows a decrease compared to thermal mode one (only a small part of the difference between ST and PVT thermal efficiency curves). The most important difference regards absorber spectral properties. While the absorber of our thermal collector shows high absorption ($\alpha = 0.92$) in the solar spectrum range and low emissivity in the infra-red spectrum ($\epsilon = 0.05$), the PV cell surface features present lower absorbance ($\alpha = 0.8$) and high emissivity. Moreover PVT has an additional thermal resistance between absorber and cells due to the additional layer of thermal paste (aluminium oxide-filled double component epoxy in the present case) used to connect the module and the absorber. The lateral heat conduction in the PV cell has an effect not so relevant due to very little cell thickness (0.26 mm). Also with this little decrease on its thermal annual efficiency, PVT panel can be very useful for domestic hot water and auxiliary heating supply if its output power is not used directly, storing it in a tank, but in aggregate with heat pump in a solar assisted single heat pump loop. Thanks to the heat pump operating temperature range, lower inlet temperatures increase heat pump operating time and so a hybrid panel is preferable with respect to a solar thermal collector. This leads to an increase on the total HVAC system efficiency (see CHAPTER 4 analysis). Different experimental analysis can be carried out with different inlet and outlet collector panel temperatures regarding PVT thermal and electric efficiency and this naturally will bring different specific efficiency results.

Chapter 4

Equation based modelling of PVT/ST panels

The work described in this chapter and in the following one has been developed during exchange research period at Fraunhofer Solar Institute in Freiburg from February to June 2012. The first research period has regarded the development of new thermophotovoltaic(PVT) and solar thermal(PVT) equation based models thanks to Dymola software (that uses Modelica language) comparing it with the old Excel working one previously developed at Fraunhofer ISE [17]in order to make it user-friendly and to obtain faster parameters analysis.

4.1 Introduction

First of all we define the notion of model: A model of a system is anything an experiment can be applied to in order to answer questions about that system. This implies that a model can be used to answer questions about a system without doing costly experiments on the real system. The term model validation always refers to an experiment or a class of experiment to be performed. The term simulation is defined like an experiment performed on a model. There are a lot of good reasons to perform simulations instead of performing experiments on real systems:

- Experiments are too expensive, too dangerous, or the systems to be investigated does not yet exist

- The time scale of the dynamics of the system is not compatible with that of the experimenter
- Variables may be inaccessible
- Easy manipulation of models
- Suppressions of disturbances
- Suppressions of second order effects to better understand primary effects

4.1.1 Dangers of simulation

It is quite easy for the user to forget the limitations and conditions under which a simulation is valid and therefore draw the wrong conclusions from the simulation. To reduce this one should always try to compare at least some results of simulating a model against experimental results from the real system.

4.1.2 Model validation

These are one of the most important things to do to verify the validation:

- Critically review the assumptions and approximation behind the model
- Compare simplified variants of the model to analytical solutions for special cases
- Compare to experimental results for cases when its possible.
- Perform sensitivity analysis of the model.
- Perform internal consistency checking of the model

With the modelization of the physical ST/PVT collector, the aim has been to test different geometries and material characteristics used in the prototype structure regarding a lot of different input conditions without building prototypes and facing with real measurement operating limitations.

4.2 Previous Excel collector model

The models compared to validate new ST/PVT Dymola models have been previously developed at Fraunhofer ISE through different Excel sheets already tested and validated with experimental results(see[17]). Using Excel sheets there are a lot of possibilities to make a model strong detailed with all input cells connected one by one with own formulas and to create easy graphs from it. But from the solving mathematical point of view there are some limitations:

- First of all (and this is one of the principal limitation) you need an external solver or use DB formulas (short for declining balance)with 3 iteration loops to solve equations and evaluate in a detailed way your model.
- Its ,for example, rather long and not easy to change quickly the geometry of the model and this limits the flexibility of the presented model.
- It is not user-friendly from the reading point of view to focus directly on components and their internal formulas. Infact you can't face graphically with your components and istantaneously click on them to change parameters.

4.3 Modelica Intro

Modelica is a modelling language that allows specification of mathematical models of complex natural or man-made systems for the purpose of computer simulation of dynamic systems where behaviour evolves as a function of time. Modelica is also an object oriented equation based programming language. The four most important features of Modelica are:

- Modelica is based on equations instead of assignment statements. This permits acasual modelling that gives better reuse of classes (equation does not specify a certain data flow direction).
- Modelica has multidomain modelling capability, meaning that model components corresponding to physical objects from several different domains (electrical, mechanical, thermodynamic, hydraulic,etc..) can be described and connected.
- Modelica is an object oriented language with a general class concept that unifies classes, generics and general subtyping into a single language construct.

- Modelica has a software component model, with constructs for creating and connecting components.

4.4 Why Dymola?

The Dymola software environment uses the Modelica modeling language which means that users are free to create their own model libraries or modify the ready-made model libraries to better match users unique modeling and simulation needs. The flexibility of Dymola makes it a versatile tool which is perfect for modeling and simulation of new alternative designs and technologies.

4.5 Our Modelica/Dymola Model

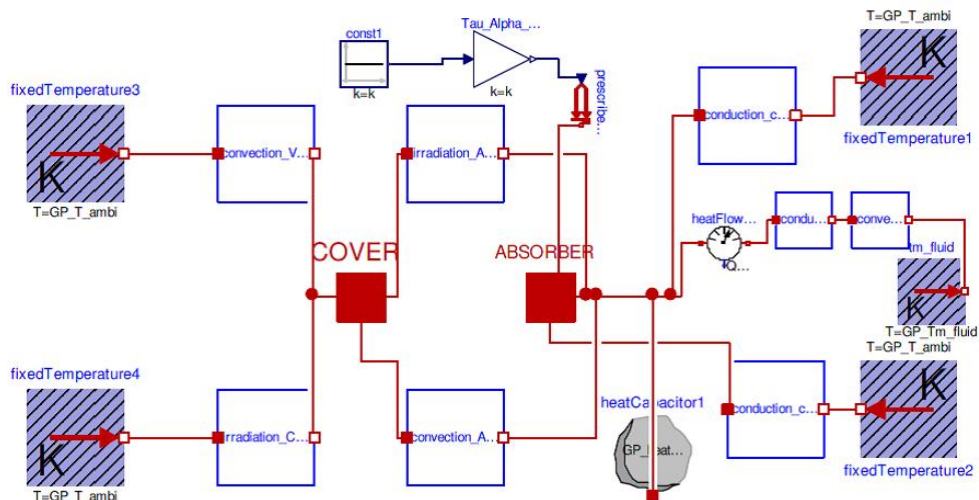


Figure 4.1: SOLAR THERMAL COLLECTOR MODEL

New ST/PVT Dymola models are developed through the Modelica language in Dymola.

At the top level you define parameters and all the other fixed values that do not change and you use in your model. The strongest possibility and feature of this model is first of all the flexibility of system modifications and subsequent collector test simulations. We are free to create our own model

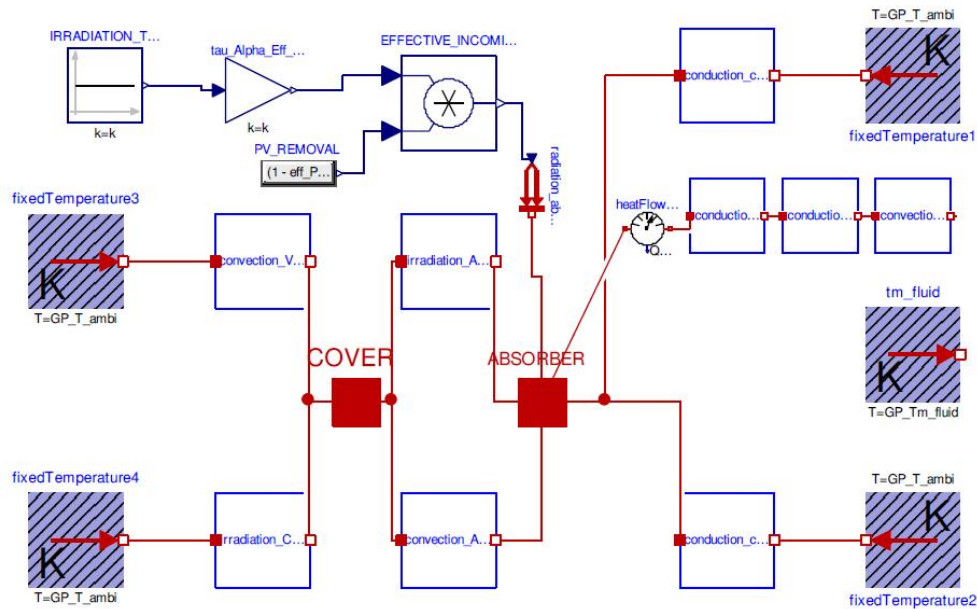


Figure 4.2: PVT COLLECTOR MODEL

libraries or modify the ready-made model libraries to better match simulation needs.

You can build new component packages or extend library ones, define model functions and use new Math blocks or extend library ones like as you can see from the graph.

If you want to change and evaluate different parameters regarding geometry factor or the properties of used material in a very quickly way, you modify all this at the top level of your code and through the equation based components you can immediately verify your output values.

```

parameter Real GP_Irr_tilt_surf=1000 "[W/m2]";
parameter Real GP_T_ambi=303 "[K]";
parameter Real GP_T_sky=0.0552*(GP_T_ambi)^(3/2) "[K]";
parameter Real GP_V_wind= 3 "[m/s]";
parameter Real GP_Teta=45 "collector tilte angle";
parameter Real GP_Spec_Coll_Flowrate=72 "[kg/hr/m2]";
parameter Real GP_Coll_Length=2 "[m]";
parameter Real GP_Coll_Width=1 "[m]";
parameter Real GP_Coll_Thickness=0.06 "[m]";
parameter Real GP_covr_solar_tran=0.902;

```

Figure 4.3: Example of Dymola code block:parameters

```

model conduction_collector_bottom "conduction collector bottom"
  extends Interfaces.Element1D;
  parameter Real Kbottom "[W/m^K]";
  parameter Real Thickness "[m]";
  parameter Real Area "[m2]";
  Real h;
equation
  h=Kbottom/Thickness;
  Q_flow = h*Area*dT;
end conduction_collector_bottom;

function f_ro_air
  extends Modelica.Icons.Function;
  input Real T_air;
  output Real ro_air;
algorithm
  ro_air:=0.000007*(T_air-273.15)^2-0.0041*(T_air-273.15)+1.2871;
end f_ro_air;

```

Figure 4.4: Example of Dymola code block:components and functions

Regarding pre and post processing input data table and graphs Dymola can also show time dependent variable combi-time table. Anyway it could be interesting for that part to use R, a free language and environment for statistical computing and graphics and import or export values to analyze.

Temporary speaking, first of all I have written the Modelica code, in order to build the solar thermal model collector, defining all the specific block packages(parameters, thermal components, functions, equations,etc..) then after little changes on geometry and effective input gain radiation, I have fixed thermal flow and efficiency calculation of the PVT one.

The validation of the Modelica model has been made through comparison with previously Excel collector model, experimentally validated, based on different sheets and DandB formulas with 3 iteration loops to solve equation models.

4.6 Differences between Solar thermal and PVT model

In these models most of the equations used to estimate the performance of solar thermal collector can be used for the thermal performance of PVT, except for this four main differences:

1. Spectral properties: The absorber of a thermal collector is usually covered with a selective low-emissivity coating. The absorbing part of a PVT collector is the PV module. The spectral properties of a PV module are different in terms of absorption and emissivity and you have to change respective parameter values of the model.
2. Photo conversion: The radiation absorbed by a PVT absorber-plate is not only converted into heat, but also into electricity because of the photo-conversion effect and you have to consider it adding a gain factor to the model.
3. Additional heat resistance: The PV, in most of PVT collector design, is mechanically and thermally connected to the top of the absorber of a flat heat exchanger. This increase the thermal resistance and is considered adding a new component.
4. Lateral heat conduction in the PV cell: The lateral heat conduction not only occurs in the absorber metal plate, but also in the solar cell itself and you can consider this with a change in the component that models collector geometry factor.

4.7 Difference between Modelica and Excel Model

Most of the equations used in the model are the same of Excel one except for the F' efficiency geometry factor. The under equation used by Excel one and derived from Duffie-Beckman(see[9]) implies U factor (thermal losses factor) knowledge and that is also a result output of simulations. That calculation is possible through the multi-loop analysis.

$$F' = \frac{1/U}{\frac{W_{tube}}{U \cdot \left(D_o + (W_{tube} - D_o) \cdot \frac{\tanh\left(\sqrt{\frac{U}{k_{abs} \cdot \delta_{abs}} \cdot (W_{tube} - D_o)/2}\right)}{\left(\sqrt{\frac{U}{k_{abs} \cdot \delta_{abs}} \cdot (W_{tube} - D_o)/2}\right)}\right)} + \frac{W_{tube}}{\pi \cdot D_i \cdot h_{fi}}}$$

Figure 4.5: efficiency geometry factor

For the Dymola model the component collector geometry factor is considered like all the others in the Q_{flow} network, so obtaining with a geometrically analysis also a thermal exchange coefficient h to evaluate it.

```

model conduction_collector_geometry
  "conduction collector geometry SHEET_TUBE"
  extends Interfaces.ElementID;
  parameter Real K_fin "[W/m^2K]";
  parameter Real Thickness_fin "[m]";
  parameter Real Length_fin "[m]";
  parameter Real Par_tubes;
  parameter Real W "distance between the tubes equal fin width";
  Real h;
equation
  h=K_fin/((W/4)-0.005)
  "conduction path length is halve of one fin width(=halve tube dist), thus halve of halve tube distance, this is per fin";
  Q_flow = h*(Thickness_fin*Length_fin^2*Par_tubes)*dT
  "for total coll times number of fins (=2x number of tubes)";
end conduction_collector_geometry;

```

Figure 4.6: Example of Dymola code block : collector geometry factor

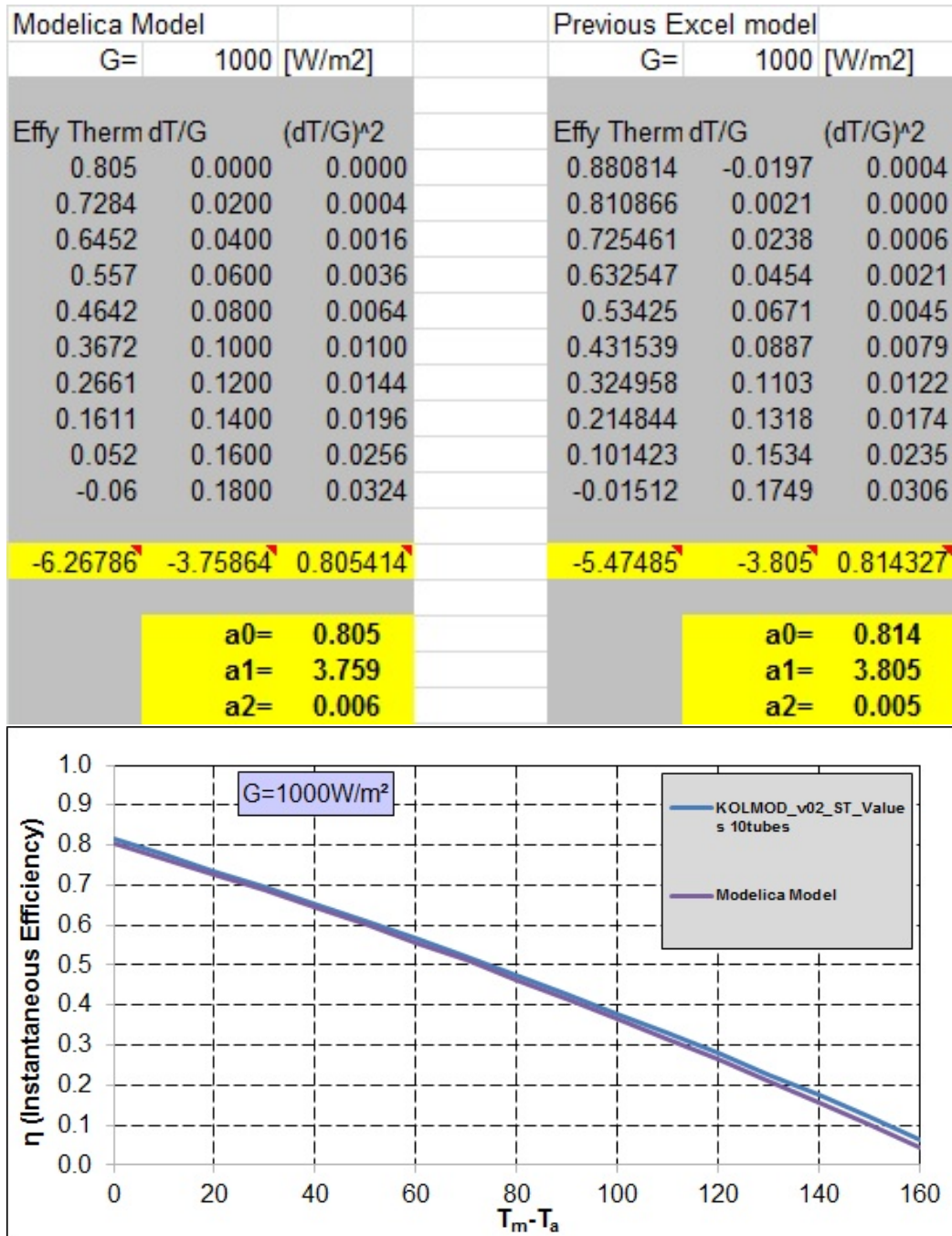


Figure 4.7: SOLAR THERMAL MODEL COMPARISON

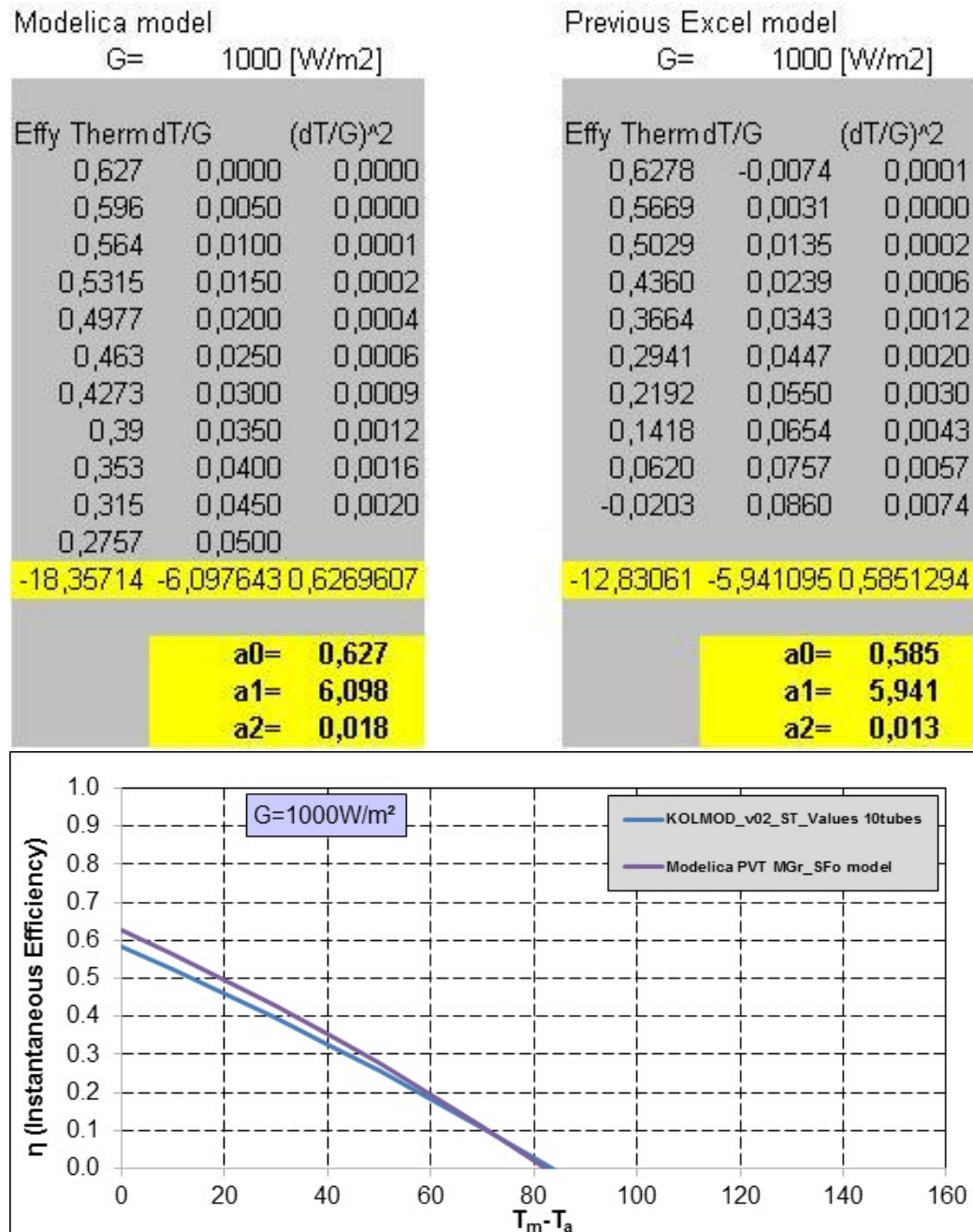


Figure 4.8: PVT MODEL COMPARISON

Chapter 5

Boundary conditions for the PVT system analysis

5.1 Description of this work package

Investigation and evaluation of different PVT system concepts consists of:

1. Elaboration of possible system variants
2. Simulation of system models
3. Assessment of the system versions

The aim of this chapter has been to identify by Polysun software possible solutions for PVT collectors and systems and to systematically compare and identify the PVT concepts which have the largest potential in solar market. System configurations have been described with advantages and disadvantages for the implementation of the concepts identified. This chapter is based on a report finalized at Fraunhofer ISE during Marcopolo PhD exchange in 2012[32].

5.1.1 Solar Heating System Performance

The performance of a solar thermal system depends in part on the performance of the solar thermal collector. The performance of a system can be judged in terms of cost performance (average *euro/kWh* over the full lifetime of the system). For solar systems this is usually done in terms of energy or cost savings in comparison to a similar conventional non-solar heating system. The savings, called F_{save} , can be expressed in end-use energy, secondary energy or primary energy saved (in *kWh/year*) or in money saved (in

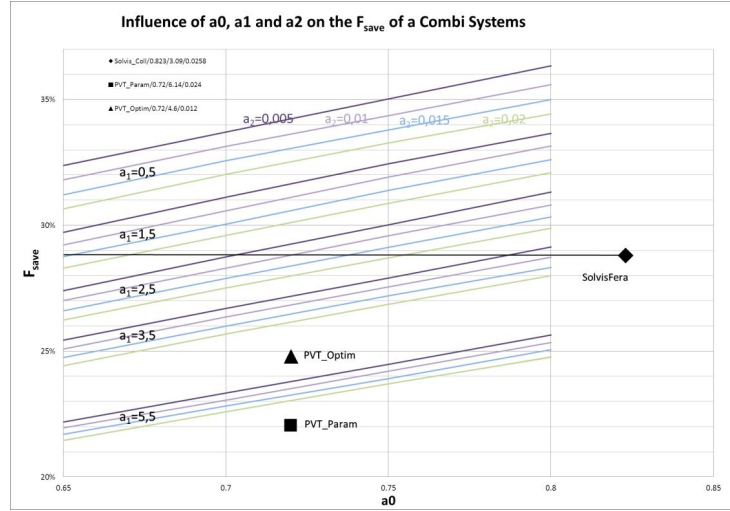


Figure 5.1: Overview of the influence of thermal collector performance parameters on the system performance (F_{save}) of a solar thermal combi-system (Fraunhofer ISE2011)

euro/year). The conventional system is often considered to be using natural gas, oil or electricity. The performance of a solar thermal collector is characterized by an efficiency curve expressed as a function of dT/G^2 . The state of art for solar thermal collectors used in domestic water and space heating is set by covered collectors which have selectively coated absorbers. They have a performance in excess of 83% (η_0 (etanull) at $dT/G=0$). These collectors have very low radiative, convective and conductive heat losses across the usual operating temperature range. In particular the radiative losses are reduced through the selective coating, leading to a first order loss factor (a_1) of $3[W/m^2K]$. Vacuum tube collectors (also with a selective absorber coating) can have an even lower first order loss factor, as low as $0.395[W/m^2K]$, due to, in addition to reduced radiative losses, almost complete suppression of convection and conduction losses. Important for market acceptance is the performance of a solar thermal system as a whole. The annual system performance is sensitive to the performance of the collectors used. The measure of a solar thermal system performance, F_{save} is sensitive to the performance parameters of the collector used. As an example, the system performance of the COMBI system depending on the performance characteristics of a collector is shown in (5.1). For this graph a lot of simulations were done at Fraunhofer ISE with different collector performance parameters a_0 (or η_0), a_1 and a_2 for a specific solar system and location.

In (5.1) also the performance of the system using commercial SolvisFera

F625I collector is indicated: it reaches a solar fraction (F_{save}) of 28.8% for this particular system (horizontal line). The graph also includes the performance of the PVTcol-project collector (previously developed by Dupeyrat in 2010 at Fraunhofer ISE) and a further improved PVT collector, both which are expected to yield less thermal savings than that of the solar thermal only collector. The graphic can be used to predict thermal savings for different collector parameters for this specific system, orientation and location (weather). For example, when the a_0 factor of the collector (product of optical $\tau\alpha_{eff}$ and thermal collector efficiency factor F') is less than 0.78, to have equal system performance as with the Solvis collector for this system the linear heat loss coefficient (a_1) has to be less than $3.5 [Wm^{-2}K]$. Or, for a value of a_1 less than $2.5 [Wm^{-2}K]$, the value for a_0 could be as low as 0.70. The latter example shows that when using a collector with an a_0 ($\tau\alpha_{eff}$) of 0.70, the same performance (as the system with the Solvis collector) can only be achieved by having a thermal loss factor of less than $2.5 [Wm^{-2}K]$ bringing the collector insulation in the range of that of vacuum tube collectors. The unit of the parameter a_1 indicates that the first order losses are proportional to the surface area (m^2) and temperature difference (K) similar to a heat transfer coefficient whereas the loss factors are proportional to the insolation (G in $[W/m^2]$).

5.1.2 Collectors Evaluated

For our Polysun simulations the following collectors are used:

- The SolvisFera solar thermal collector
- The PVT collector from Project PVTcol
- An uncovered PVT collector
- An improved (not optimized) PVT collector

The performance of a solar thermal collector is characterized by its efficiency as a function of dT/G . This curve is described by three parameters and a given insolation (G). The performance parameters of collector used in this research are given in Table 5.1.

Additional collector field parameters used in the simulation:

- Collector orientation: South, Inclination 45° , no shadow, Weather: Passau;
- Heat transfer fluid: water, specific flow rate: $72kg/hm^2$, Piping: 10 m;

- Controller: Differential, On: 7°C, Off: 4°C;

The influence of the wind on the collector performance varies strongly: from a large influence on uncovered collectors, to hardly any influence on covered collectors. Because the actual wind on the collector depends on many specific local factors (tilt, height, orientation, surrounding wind-shading or enhancement, and often unknown local wind speeds over time) a constant average wind condition of 3 m/s is taken for simulations. The performance parameters here are all measured with an average 3 m/s wind speed. The performance graphs of each collector at an insolation of $1000W/m^2$ and wind speed of 3 m/s are shown in (5.2). The graphic also gives an indication of the maximum stagnation temperature of the collector.

Values are based on the aperture area of the collector. Graph only applies to operation under the indicated irradiation intensity and under $3m/s$ wind. The thermal and electrical performances of a PVT collector depend on the following ambient factors:

1. Ambient temperature. Higher ambient temperature means:
 - Higher thermal performance
 - Lower electrical performance
2. Insolation. Higher solar insolation means:
 - Higher thermal and electrical performances
3. Wind Higher wind speeds means:
 - Lower thermal performance
 - Higher electrical performance

These factors are location specific and none can be influenced by altering the system configuration. In the following chapter the only system factor that can be influenced by the solar heating system configuration is discussed.

Collector Parameters	a0	a1	a2
SolvisFera	0,823	3,09	0,0258
covered PVT collector	0,72	6,14	0,024
uncovered PVT collector	0,7	20	0,02
Improved PVT collector	0,72	4,6	0,012
PV module	0,3	8,3	0,04

Table 5.1: Collector parameters used in our Polysun simulations

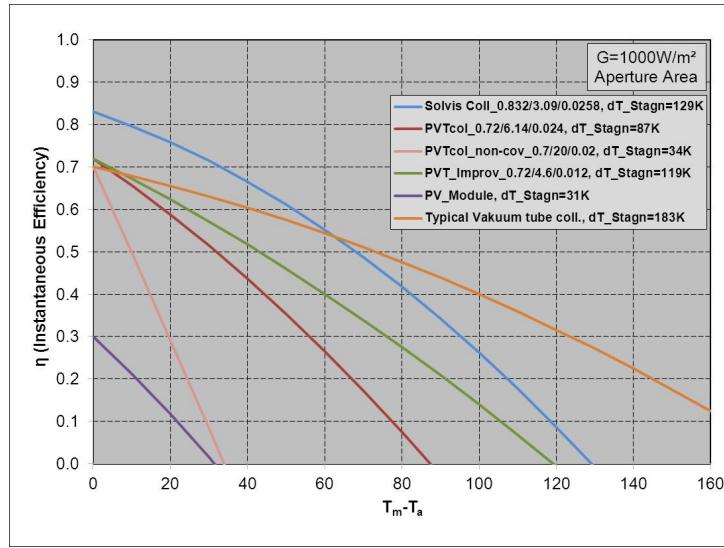


Figure 5.2: Collector performance graphs of the considered collectors. (η_t = instantaneous thermal efficiency, T_m = medium collector temp, T_a = ambient temp, G = Irradiation (Fraunhofer ISE2011))

5.1.3 Systems evaluated

In order to determine suitable system concepts for use with PVT collectors the aim is to identify relevant and beneficial system configurations. Also important is that systems in this analysis are also chosen because they are market relevant or they may be promising particularly for PVT applications. The analysis here focusses on the thermal yield of solar thermal systems operating with flat plate PVT collectors compared to systems operating with conventional flat plate solar thermal (ST) collectors. The difference in thermal performance depends mainly on the following single, controllable system factor: the temperature of the fluid flowing into the collector inlet (T_{inlet}). A higher inlet temperature leads to a lower (instantaneous) thermal efficiency of the collector. A lower instantaneous efficiency at the operating point (dT/G or dT) leads to a lower energy yield by the collector. The influence of an improved system configuration with reduced inlet temperature can be deduced from the slope of the collector efficiency curve: a collector with steeper efficiency slope (higher thermal loss factors) should benefit more from a reduced inlet temperature than a collector with lesser slope. It is however not beneficial to operate the collector loop pump at very low efficiencies as this requires pumping energy and causes excessive disturbances in the stratification of the tank which may undo the benefit of operation at this low efficiency. Thus collectors should not operate at too low efficiencies. Usually an insolation

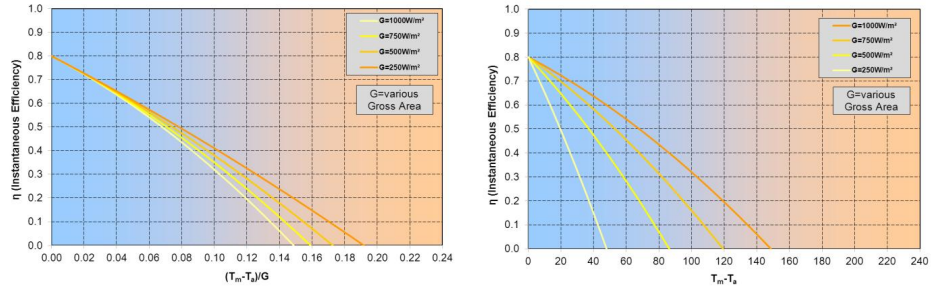


Figure 5.3: Influence of insolation levels on the instantaneous efficiency of a solar thermal collector (two different efficiency representations: dT/G (left) and dT (right))(Fraunhofer ISE2011)

threshold of $150W/m^2$ is used for pump operation to commence. (5.3) shows the instantaneous efficiency curves of a solar thermal collector for different insolation levels (two different efficiency representations are shown: dT/G and dT). The effects of different insolation levels on efficiency curves shown are similar for any solar thermal collector. This leads to the following comparison of benefits of reducing the inlet temperature, illustrated in (5.4).

In (5.4) efficiency curves of two collectors are given at two different insolation levels.

(5.4) also shows two system improvements made which led to a reduction in collector inlet temperature, and thus a reduction in dT . For $dT1$ the efficiency of the PVTcol collector increases more than that for the SolvisFera collector, because the efficiency curve for the PVTcol is steeper. But for improvement $dT2$, the efficiency and yield from the Solvis Fera increases while the efficiency of the PVTcol collector still does not reach the threshold. The first system improvement means that the annual system yield from the PVTcol will benefit more from the system improvement than that from the SolvisFera collector. In the latter this means that the annual system yield of the system with the SolvisFera will increase while that from the PVTcol collector does not change. This latter difference is expressed as a reduced operating time for the lesser performing collector, leading to a comparatively much reduced annual yield of the lesser performing collector. This means that although the efficiency of a collector with higher loss factor may benefit more from a system improvement (i.e. lower collector inlet temperature) the annual yield of that system often does not. The annual benefit depends also on the distribution of the annual operating conditions. Consider a distribution of potential operation conditions along the x-axis (operation conditions defined by T_{coll} mean, T_{ambi} and G). Opportunity losses increase when operat-

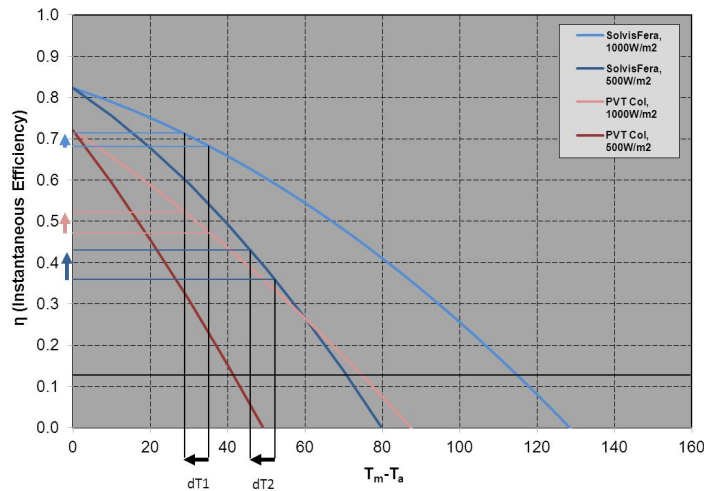


Figure 5.4: Difference in benefit of reducing the inlet temperature for collectors with high and collectors with low heat loss factors, for two different insolation levels ($1000W/m^2$ and $500W/m^2$). The line at 0.13 efficiency indicates an efficiency threshold (Fraunhofer ISE2011)

ing conditions are outside the range of effective operation of the collector. A collector with higher loss factors not only loses annual yield due to a lesser instantaneous operating efficiency but it also loses yield due to increased opportunity losses defined by occurrences of conditions outside effective operation of the collector. The inlet temperature can be influenced by the system configuration. For systems with stratified storage this factor is directly determined by the temperature in the store at the level from which the collector is supplied. For many solar thermal system is pays to stratify the store to reduce the collector inlet temperature. In the case of a non-stratified store this temperature is equal to the overall store temperature. The latter is possibly determined by the temperature setting of the auxiliary heating. Pre-heat systems, which do not apply an auxiliary heater inside the solar storage tank, are in any case beneficial over systems in which the auxiliary heater increases the inlet temperature of the collector.

A store is operated with charge and discharge loop or open connection pairs (double ports), for stratified tanks a warm connection is above a colder connection. For discharging connections/loops (DHW connections and the space heating loops) the higher placed warm connection is an outlet from the store and the colder lower connection an inlet into the store (i.e. a return connection). For charging loops (e.g. solar loop and auxiliary loop) the warm (upper) connection is an inlet into the store and the colder (lower)

connection an outlet from the store. A DHW system can be designed as a flow through system (without a return flow) and thus the store temperature is then influenced by the incoming cold mains water temperature. For all other configurations, the store temperature is influenced by the temperature of return flows. Stratification is disturbed by charging and discharging, in particular due to high mass flow (in particular for open inlets), non-matching temperatures between the store temperature and that of the connected flow, as well as through high temperature auxiliary heating devices inside the store. Return flow rates and temperature differences, need to be kept low to allow stratification to be maintained.

A recent paper by Glembin and Rockendorf [31] researched the influence of stratified charging and discharging in Combi systems (see also [30]). The main conclusion from the paper is reproduced here: the results of this study show that a good thermal stratification within the storage and thus higher energy savings can be reached by both a stratified charging and discharging. Depending on the system size and the design of charging and discharging connections the stratified discharging leads to the same or even higher energy savings than a stratified charging. Already one single four-way mixing valve in the space heating flow (i.e. two tapping points) leads on the one hand to more than 80% of the advantage of an idealized discharging with seven tapping points, and on the other hand in all cases to significantly higher energy savings if compared to two charging devices with three-way valves. The relative energy savings increase with increasing solar fraction, e.g. with larger dimensions and better insulated buildings. The best option with the highest benefit depends on the system design like storage in- and outlet positions, system size and load conditions. Therefore, the decision for the best suited strategy can only be determined by simulations representing the respective system [31]. The following flow control strategies as well as stratifying aids can be used for the solar loop or space heating loop. The energy supply in the collector loop varies as the irradiation on the collector varies. The control strategy for collector loop to adjust to this variation is called matched flow. With matched flow in the collector loop the flow rate (pump speed) is adjusted to the insolation and/or to a desired return temperature. However this configuration requires additional sensors and a pump with controllable variable flow. For space heating loops beneficial control strategies include the use of a stratified return for the space heating loop (or four-way valve, see conclusion of [31]).

Stratifying aids include:

- Flow limiters which limit the maximum flow rate, in kg/h and flow diverters both reduce mixing in the tank.

- Stratification lances and internal heat exchange covers.

The latter promote the stratification in the tank by allowing the heated liquid to flow to the layer with the similar temperature (actually: through the gravitational effect of the changing water density with temperature). For combi systems, achieving higher solar fractions requires storing energy for longer periods (e.g. from weeks up to several months in seasonal storages) due to the temporal mismatch of available solar radiation (in summer) and periods of high heating demand (in winter). Although large storage tanks have the potential (side) effect of lowering the collector inlet temperature the requirement to store large amounts of heat and the addition of return flows with temperatures above the cold water mains temperature means that the performance is usually lower for combi systems than for DHW systems. Large Fsav systems are included in this analysis based on the likely growing market for these systems. A distinction is made between systems with large stores ($< 10m^3$) and systems with seasonal storage (e.g. $> 10m^3$) as well as different housing concepts: a conventionally insulated house (ca. $100kWh/m^2y$), a low energy house (ca. $50kWh/m^2y$) and a very low energy house ($< 25kWh/m^2y$). An often mentioned configuration is the combination of PV modules with a heat-pump. The point is that the electricity needed for heat pump operation can then be delivered by the PV panels (considering the temporal mismatch). Alternatively PVT or ST collectors can operate with PVT collectors in direct thermal connection with a heat-pump (so called solar assisted heat pump systems or SAHP). The heat-pump then provides extra cooled liquid to the collector and extracts the heat from the collector loop fluid. The PVT collector can then operate at reduced inlet temperatures, and thus potentially higher efficiency, as well as for the heat pump which can extract heat at higher than ambient temperatures. However there are tight limitations for this configuration in particular regarding the temperatures at which a heat pump can operate due to the limited operating pressure range of the heat pump evaporation liquid. Too high and too low temperatures prevent the heat pump from working effectively (see Table 5.2). To limit the temperature range of the supply and to provide some storage a borehole is used between the collector and the heat pump. This system configuration is however outside the budget of most single family homes, and forms thus only a small niche market .

When these ranges are exceeded the heat pump is stopped. When collector outlet temperatures are exceeded it is then possible to by-pass the heat pump and feed the heat directly to the storage tank or for use in the space heating loop. The limitations make the combination of heat pump with non-covered PVT modules which have much lower operating temperatures

	Supply side inlet	Demand side outlet
Min.	-5	65
Max.	25	90

Table 5.2: Heat pump inlet and outlet temperature limitations

interesting. The following system-configurations are of interest to determine suitable system concepts for use with PVT collectors (indicating services provided and auxiliary heating method used):

- Domestic hot water (DHW) flow through systems for single family houses (SFH) and multi-family houses (MFH); Variants: preheating (flow-through heater) and auxiliary (store) heated systems.
- Combi-systems providing support for both domestic hot water and space
- Variants: stratifying aids and different space heating loop configurations.
- Large solar thermal stores: i.e. Combi-systems providing a large fraction of both domestic hot water and space heating demand (but with store volume less than $10m^3$).
- Large solar fraction houses with seasonal heat stores; Solar Assisted Heat-pump systems (SAHP) which use a (covered or non-covered) PVT collector as a heat source.

5.2 System Analysis

The systems used in the Polysun simulations include:

- A flow through DHW pre-heat system (DHW)
- An auxiliary heated Combi-system (Combi)
- A large solar fraction system (SF-House)
- A solar assisted heat pump system (SAHP)

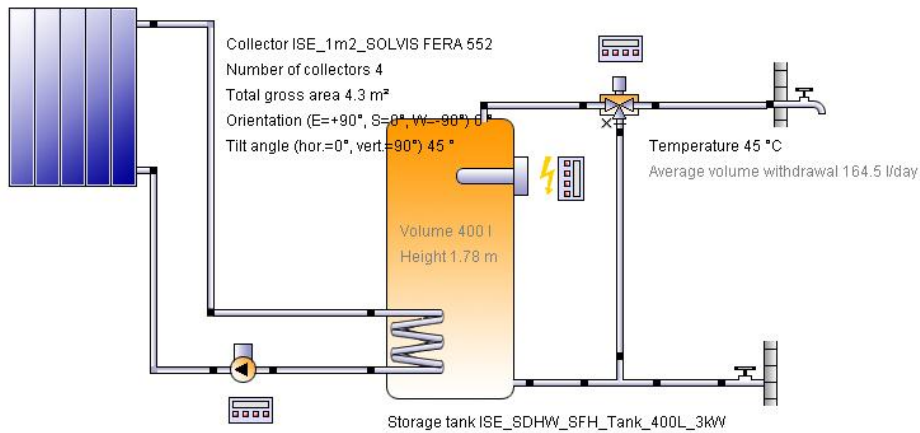


Figure 5.5: Scheme of the flow through DHW pre-heat system configuration

5.2.1 Flow through DHW pre-heat system (DHW)

A summary of settings for the DHW-system simulation is given below.

- Collector field: For collector parameters see Table 5.3.
- Mass flow rate: depending on insolation (a maximum of $72\text{kg}/\text{hm}^2$ at $1000\text{W}/\text{m}^2$, starting at $150\text{W}/\text{m}^2$).
- Water storage: Reference system with 300 litre tank, electrically heated drinking water tank;
- Solar system : storage tank of 400 litre, with built-in electrical auxiliary heater at 70% of the store height of 1.78 m, or an external on demand continuous flow heater before the tap.

The demand is determined by 175 l/day at 45°C with 3 weeks of holiday per year (15 – 29th July and 22 – 27th December). This results in 165, 4l/day average demand, and 2460 kWh/year (end-use) DHW energy demand. The annual thermal yields of different collectors in a SDHW system are compared using Polysun simulation software. The relevant criterion for this comparison is: annual fractional (end-use) energy savings: $F_{save}[\%]$.

SDHW System Variations

The following variations in the solar domestic hot water (SDHW) systems were made for analysis purposes:

- Different collectors: standard well performing solar thermal collector (ST), covered photovoltaic-thermal hybrid collector (PVT), improved covered PVT collector and uncovered PVT collector.
- Different collector areas: 4m^2 and 6m^2 , and a full range of 4 - 30m^2 , as well as the collector area needed for equivalent F_{save} .
- Different auxiliary heating settings: Set-points at $52,5^\circ\text{C}$ and $62,5^\circ\text{C}$, as well as a solar preheat only (with continuous flow heater demand) configuration.

SDHW System Results (Thermal only)

The results of the system simulation for the SDHW systems with variations in collector type, collector area and auxiliary heaters are shown in Figure 5.6.

From (5.6) it can be concluded that: A change from 4m^2 to 6m^2 does not increase the yield proportionally, but only 10-11% for covered collectors and very little (1-2%) for uncovered PVT collectors (see equal F_{save} analysis below). The thermal yield of the uncovered PVT collectors can be ruled insufficient for use of these collectors in auxiliary heated SDHW systems. The use of the solar pre-heat system configuration (with continuous flow heater before the tap) is still most beneficial for the non-covered PVT collectors, but the yield is still doubtfully low. The covered PVT collectors also achieve a much lower yield than the ST collectors. A lower auxiliary heater set point, e.g. $52,5^\circ\text{C}$ instead of $62,5^\circ\text{C}$, is clearly beneficial for SDHW systems, even more for PVT collectors than ST collectors. A reduction of the auxiliary set point is recommended for auxiliary heated SDHW SFH systems which use (covered) PVT collectors. The continuous flow heater systems provides the best yield increase for the PVT collectors and is the preferred option for SDHW systems with PVT collectors. In (5.7) and (5.9), using multiple simulations, the relationships between collector area and F_{save} are shown for

Collector Parameters	a_0	a_1	a_2
SolvisFera	0,823	3,09	0,0258
covered PVT collector	0,72	6,14	0,024
non-covered PVTcoll	0,7	20	0,02
Improved PVT collector	0,72	4,6	0,012
PV module	0,3	8,3	0,04

Table 5.3: Collector performance parameters used in Polysun simulations.

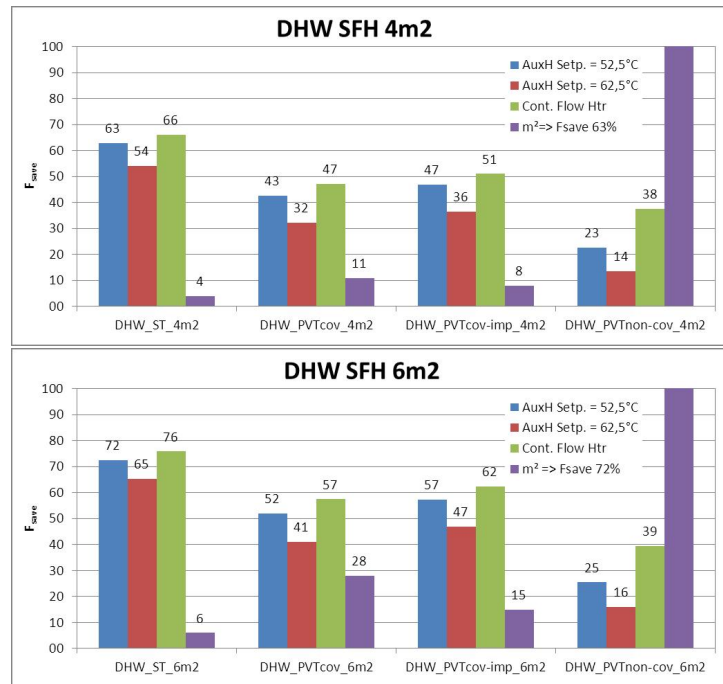


Figure 5.6: Results for the SDHW system with collector type and auxiliary heaters variations for collector area of $4m^2$ and $6m^2$

different collectors. The required collector area for achieving the same F_{save} for different collectors can also be determined from these graphs. The collector areas required for the F_{save} of 60% (horizontal black line) are indicated in the figures (vertical black lines).

From (5.7-5.8-5.9) it can be concluded that an F_{save} equal to that of 4 or $6m^2$ of ST collectors (63.0%*resp.*72.5%) cannot be achieved with the PVT uncovered collector. If the slope of the curve is an indication of the economic feasibility of marginally adding collector area (i.e. when it is still economically beneficial to add collector area because the yield still increases strongly by doing so, assuming equal per area cost of the collectors) then the optimum collector area is smaller for lesser performing collectors (compare the slope of curves at equal F_{save}). A comparison between the auxiliary heated and pre-heat system graphs also shows that the optimum for the pre-heat system is reached at larger collector areas than for the (52.5°C) auxiliary heated system. This means that systems with larger collector area benefit more from the continuous flow heated /solar pre-heat system. Pre-heating systems are thus in particularly preferred for larger collector areas. Often certain savings are aimed for, in the case of SDHW for example an $F_{save} = 60\%$ is often taken as a guiding number (a balance between cost of

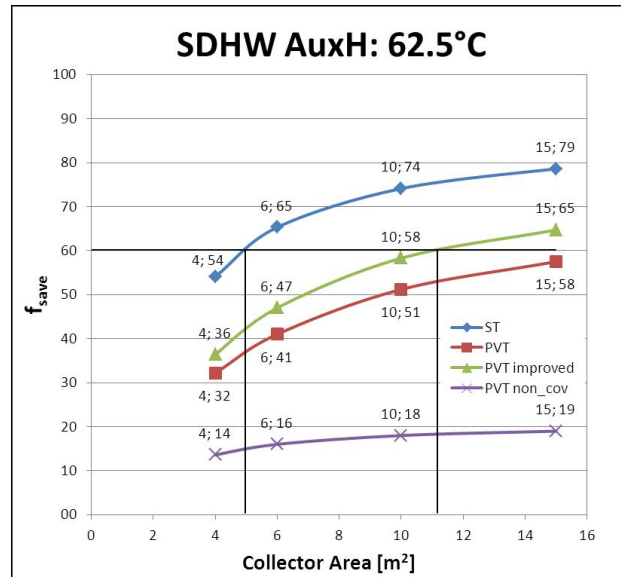


Figure 5.7: Results for the auxiliary heated SDHW system (set point of 62.5°C) with varying collector area for different collectors

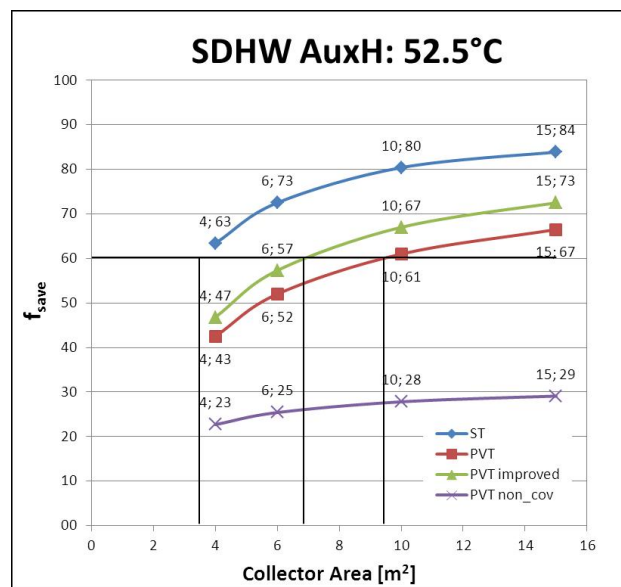


Figure 5.8: Results for the auxiliary heated SDHW system (set point of 52.5°C) with varying collector area for different collectors

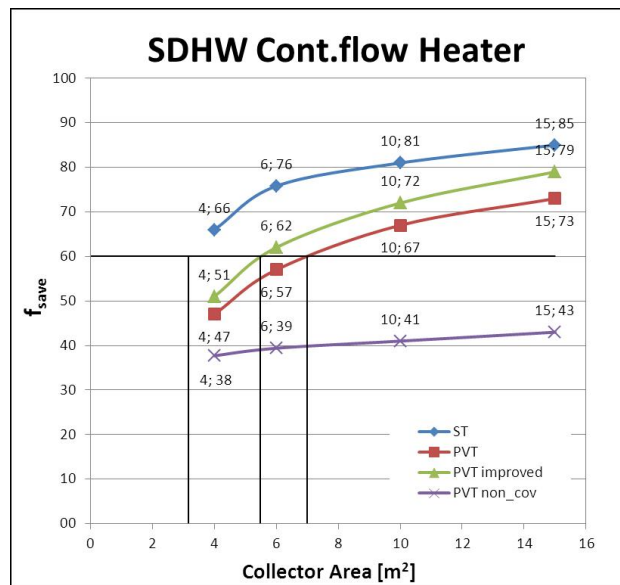


Figure 5.9: Results for the pre-heat SDHW system (continuous flow heater) with varying collector area for different collectors

the system and usability of the collectors). In Table 5.4, the values for the required collector areas (vertical lines in 5.7-5.8-5.9) are given for achieving this level of savings.

From 5.4 it can be seen that:

- Using a continuous flow heater in a pre-heat SDHW system combination is more beneficial for the PVT collector (18% and 26% reduction in collector area) than the ST collector (7% reduction)
- For achieving a thermal (only) performance comparable with ST (only) collectors, double the collector area of improved PVT collector is required.

Coll. Area	Aux. heater set point: 62,5°C	Aux. heater set point: 52,5°C	Continuous flow heater	Diff. Area (62.5°C and Cont.Flow)
ST	4.9	3.5	3.2	34
PVT	16.8	9.3	6.9	159
PVT impr	11.1	6.8	5.6	50

Table 5.4: Collector area required for achieving an F_{save} of 60% for the SDHW systems (values rounded)

- By improving the solar heating system (using a solar pre-heat system instead of an auxiliary heater with set point at 62.5°C) the improved PVT collector can achieve the $60\%F_{save}$ with only a 13% larger collector area (5.6m^2 instead of 4.9m^2), keeping in mind that the PVT system also generates electricity at an efficiency of 15%, this is a major improvement
- Comparing like-for-like, or applying the same continuous flow heater to the ST system the area increase from ST to PVT is 73%.

A comparison of the graphs in (5.10) shows the influence of the auxiliary store heating on the collector and store temperatures: The collector inlet temperature (red), collector outlet temperature (black) and collector operating temperature (green) are all higher for the auxiliary (store) heated system, thus the collector operating efficiency in this system is lower. In addition it can be seen that the operating times (width of the green activation curve) is generally narrower for the auxiliary heated system. The latter indicates that this system has higher system opportunity losses .

A comparison of the graphs in (5.11) (both pre-heat systems with 4 resp. 6 m^2 of non-covered PVT collectors) shows the slightly higher temperatures (collector inlet temperature (red), collector outlet temperature (black) and collector operating temperature (green)) and (sometimes) slightly shorter operating times (green line) for the system with larger collector area. Although the available solar radiation is larger for the system with larger collector area, the much reduced collector efficiency due to slightly higher operating temperatures compensates this benefit and prevents a significant increase in annual yield.

(5.11) also shows non-operating solar loops in the first two days due to low insolation. Compared to the operating times in the graphs of the covered PVT collectors (compare with (5.10) this shows a significant opportunity loss for the system with non-covered collectors, explaining the much lower annual yield of the non-covered collectors. (5.12) shows that the collector energy yield (red line) is generally a little higher in the pre-heat system temperature, while the auxiliary heating energy (black) is slightly higher for the auxiliary heated system. The temperature at the top of the tank (purple) can be seen to follow the available solar radiation in the pre-heat system where as for the auxiliary heated system it is consistently high.

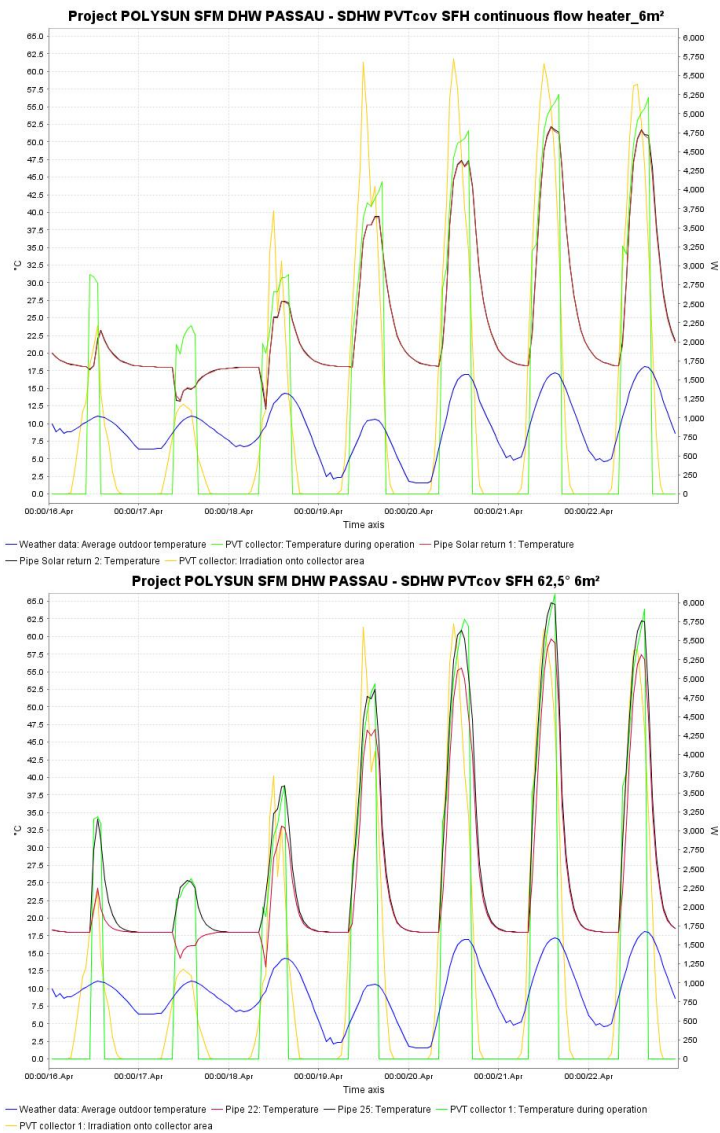


Figure 5.10: Two graphs with temperature curves of the SDHW Pre-heat (top, $F_{save} = 57\%$) and auxiliary heated systems (bottom, $F_{save} = 41\%$) using covered PVT collectors, for a week in mid-April, showing: ambient temperature (blue), amount of radiation on the collector area (yellow), collector inlet temperature (red), collector outlet temperature (black), collector operating temperature (green)

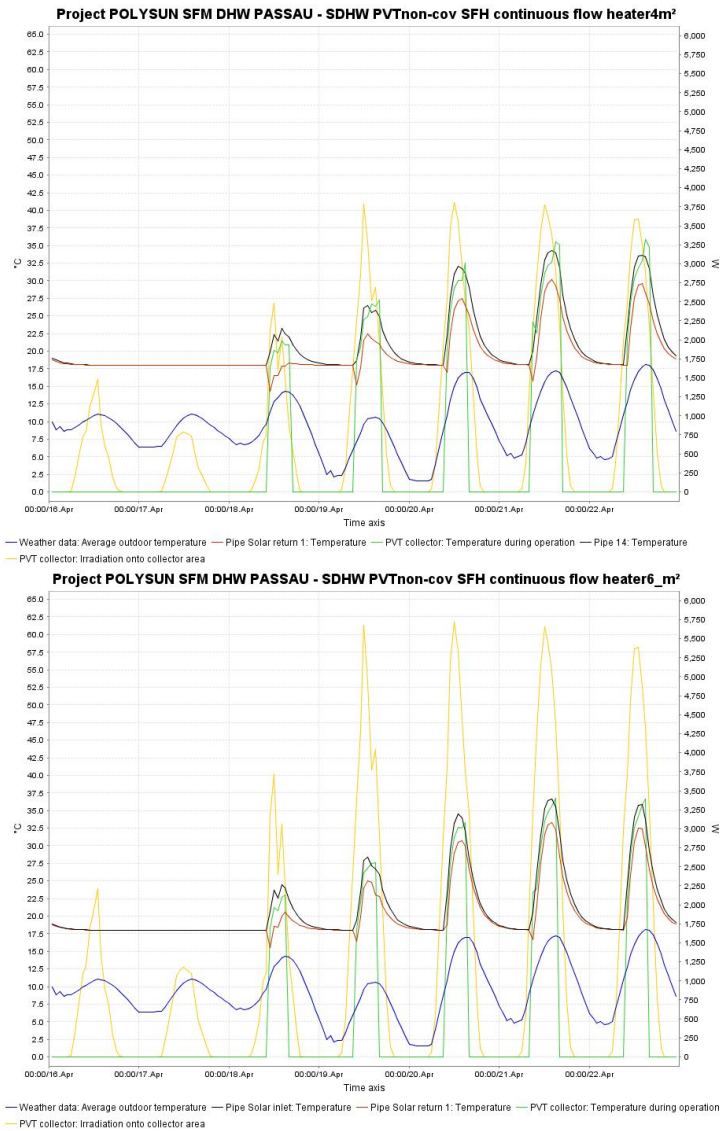


Figure 5.11: Two graphs with temperature curves of the SDHW (pre-heat) continuous flow heated system using either 4m^2 (top, $F_{save} = 38\%$) or 6m^2 (bottom, $F_{save} = 39\%$) of non-covered PVT collectors, for a week in mid-April, showing: ambient temperature (blue), amount of radiation on the collector area (yellow), collector inlet temperature (red), collector outlet temperature (black), collector operating temperature (green)

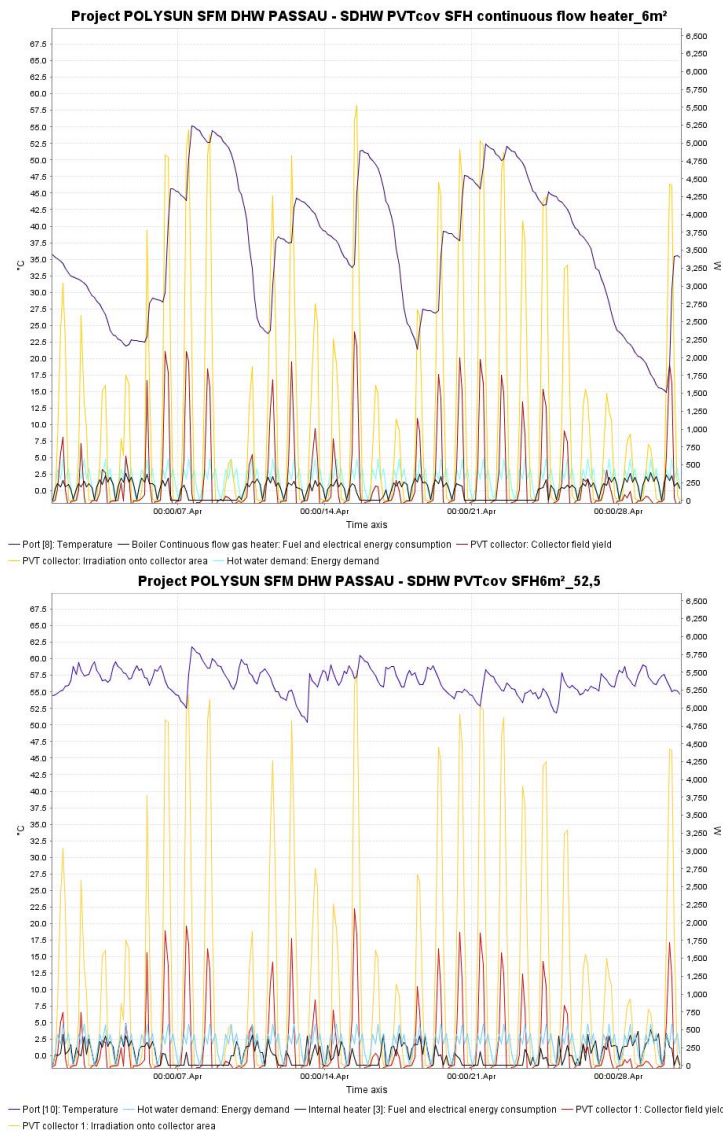


Figure 5.12: Two graphs with temperature and energy curves of the SDHW pre-heat (top, $F_{save} = 57\%$) and auxiliary heated systems (bottom, $F_{save} = 52\%$) using covered PVT collectors, for the month of April, showing: temperature (left axis) at the top of the tank (purple), amount of (energy, right axis) radiation on the collector area (yellow), collector energy yield (red), auxiliary heating energy (black), DHW energy demand (light blue)

5.2.2 Auxiliary Heated Combi System

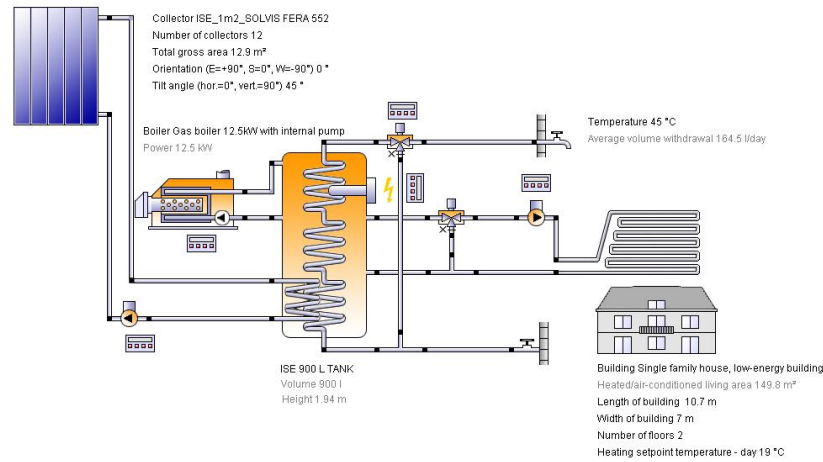


Figure 5.13: Scheme of the auxiliary heater Combi system configuration

A summary of settings for Combi system simulation(5.13)is given below:

- Collector field:South orientation, inclination 45°, no shadow, Weather:Passau.
- Collector parameters:see Table5.3(the same as for SDHW system).
- Mass flow rate: depending on insolation, a maximum of 72kg/hm² at 1000W/m², starting at 150W/m².
- Storage tank: Reference system with 900 litre tank, electrically heated water tank.Solar system storage: tank of 1000 litre, with built-in electrical auxiliary heater at 70% of the store height of 2m.
- DHW : Internal heat exchanger pipe in tank.
- DHW consumption: demand determined by 175l/day at 45°C;3 weeks of holiday (15–29th July and 22–27th December). This results in 165,4l/day average demand and 2460 kWh/year(end-use)DHW energy demand.
- Space heating: The demand is determined by a standard single family house (SFH) of 150m² with different specific heating energy demand: normal house (105kWh/m²year), low energy house (55kWh/m²year) and very low energy house (23kWh/m²year).

The annual thermal yields of different collectors in a Combi system are compared using Polysun simulation software. The relevant criterion for this comparison is: annual fractional (end-use) energy savings $F_{save}[\%]$.

Combi System Variations

The following variations in the solar domestic COMBI system were made for analysis purposes:

- Different collectors: standard well performing solar thermal collector (ST), covered photovoltaic-thermal hybrid collector (PVT), improved covered PVT collector and uncovered PVT collector.
- Different collector areas: 12,18,30,42,50m².
- Different auxiliary heating settings: Set-points at 52,5°C and 62,5°C.
- Different collector mass flow (control) strategies: Default (radiation dependent) Matched Flow (temperature matching in store) Stratified return flows.
- Different hydraulic scheme geometries.

Combi System Results (Thermal only)

The results of the system simulation for the Combi systems with variations in collector type, collector area and auxiliary heaters are shown in(5.14-5.15):

From (5.14-5.15) can be concluded that the annual yield of the system with PVT collectors is 1/3 (for 52,5°C) to almost 1/2 (for 62,5°C) less than that of the one with solar thermal only collectors. Through reducing the auxiliary heating temperature and lowering the heating demand, the difference between the energy yield from the ST and PVT collectors can be reduced from 41-47% to 30-35%. The use of a lower auxiliary heating setting is more beneficial for the system with PVT collectors and becomes increasingly more beneficial with reduced heating demand. The largest differences are between systems using ST and PVT collectors in the normal energy house with high auxiliary heating setting and also between the systems with different auxiliary heating temperatures for the very low energy houses using PVT collectors. (5.14) shows also that although the solar thermal only collectors operate at much higher temperatures (ca. +20°C) it does not mean that this happens at lower efficiencies, which is indicated by the varying shorter and longer operating times.

(5.16) shows that the (large) difference in yield between the Combi systems using PVT collectors with auxiliary temperature setting 62, 5°C (top, $F_{save} = 24\%$) and 52, 5°C (bottom, $F_{save} = 29\%$) is caused by differences in collector operating efficiency due to different collector operating temperatures of 2, 5 ÷ 5°C higher, although the operating times are similar (thus not

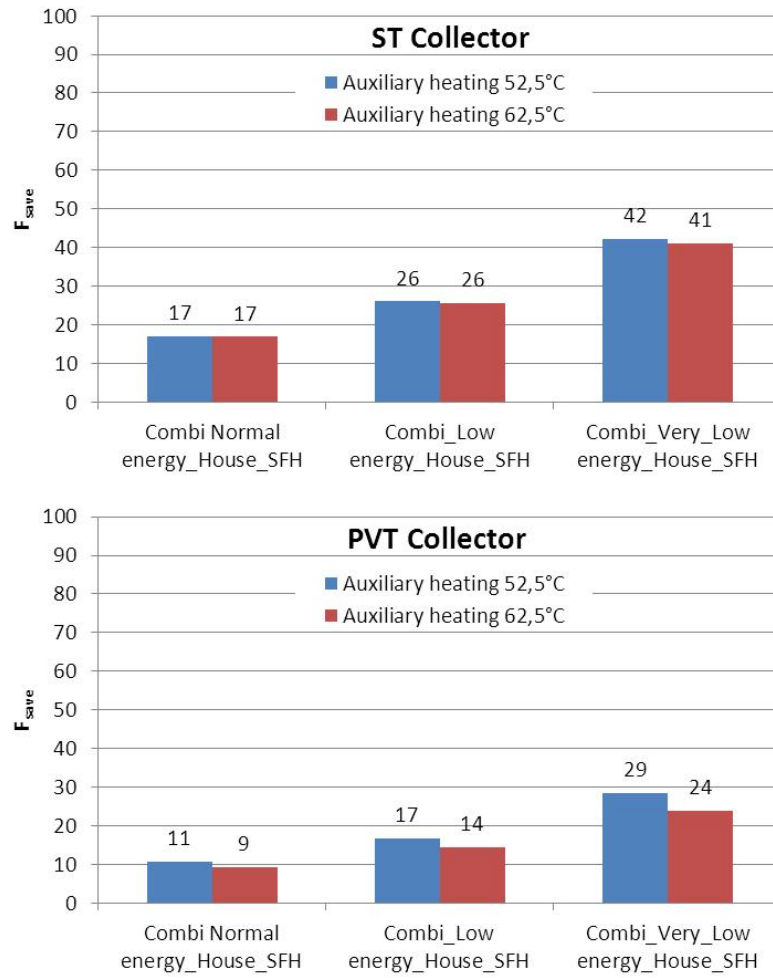


Figure 5.14: Results for the Combi system with solar thermal collector (left) and PVT collector (right) (all 12m²), for two different auxiliary heating settings

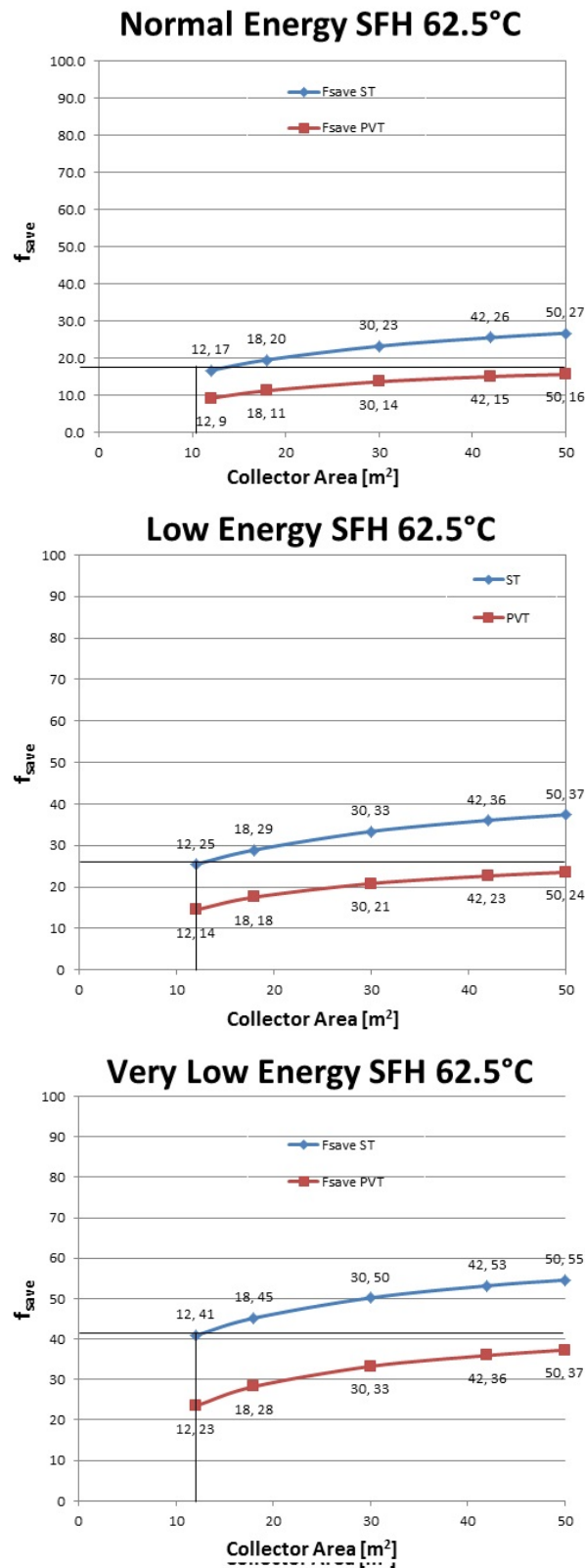


Figure 5.15: Results for the Combi system with solar thermal collector and PVT collector with different areas from 12 to 50m² and auxiliary setting temperature 62.5°C

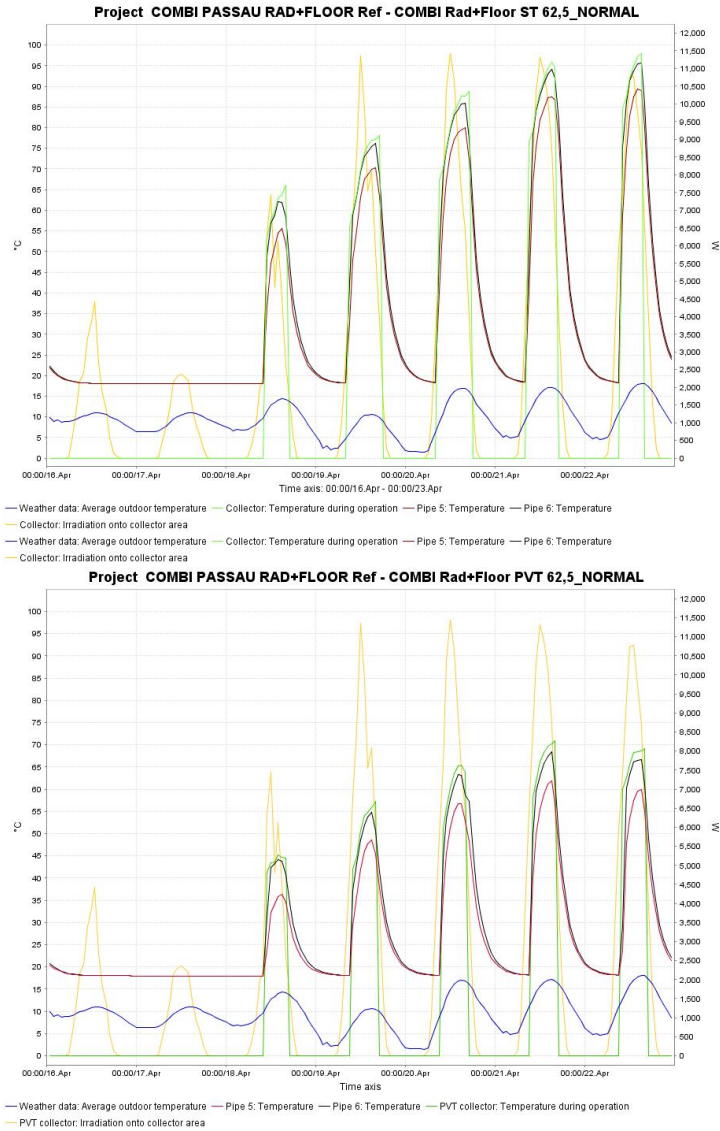


Figure 5.16: Two graphs with temperature curves of the auxiliary heated Combi system (temperature setting $62,5^{\circ}\text{C}$) with 12m^2 collector area using either solar thermal collector (top, $F_{save} = 17\%$) or PVT collector (bottom, $F_{save} = 9\%$), for a week in mid-April, showing: ambient temperature (blue), amount of radiation on the collector area (yellow), collector inlet temperature (red), collector outlet temperature (black), collector operating temperature (green)

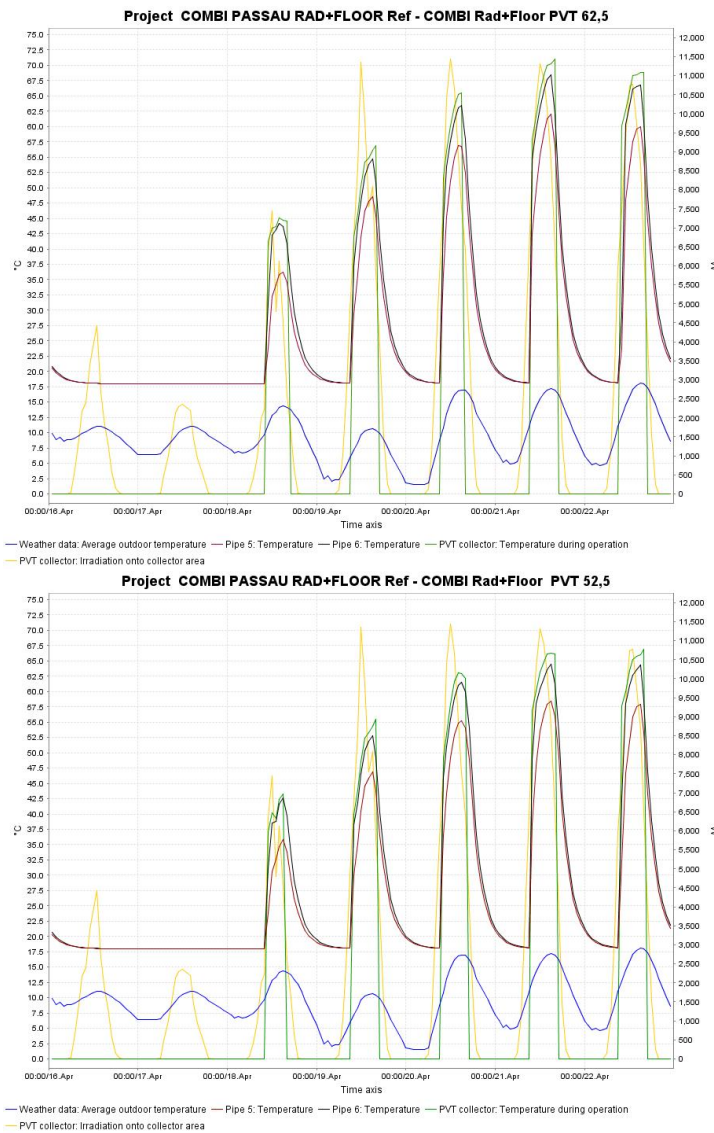


Figure 5.17: Two graphs with temperature curves of the auxiliary heated Combi system using a PVT collector with auxiliary settings $62,5^{\circ}\text{C}$ (top, $F_{save} = 24\%$) and $52,5^{\circ}\text{C}$ (bottom, $F_{save} = 29\%$), for a week in mid-April, showing: ambient temperature (blue), amount of radiation on the collector area (yellow), collector inlet temperature (red), collector outlet temperature (black), collector operating temperature (green)

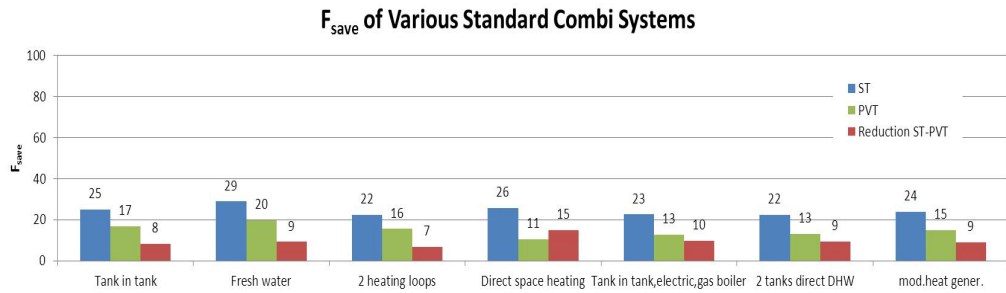


Figure 5.18: Results of 7 different (standard) Combi systems using PVT or ST collectors and the low energy house demand. The differences in yield are shown in the red columns. Flow control: Radiation dependent

caused by a difference in opportunity losses). From this it can be concluded that for Combi system:

- A reduction in the auxiliary temperature setting is beneficial for all systems and in particular for those with PVT collectors because it leads to higher operating efficiencies.
- A larger imbalance between energy supply and demand (quantitatively and temporal) is only slightly more detrimental for the system with PVT collector than with solar thermal collector.

The results of 7 different (standard) Combi systems are shown in (5.18). The yield varies strongly per system, from $F_{save} = 22\%$ to 29% for systems with ST collectors and from 11% to 20% for systems with PVT collectors. The red columns show that the differences in yield between ST and PVT are not always proportional to the yield itself: sometimes the change from ST to PVT causes a small (7%) drop in performance and sometimes a large (15%) drop. The size of which is unrelated to the ST system performance (26 resp. 22).

Many more system factors play a role in the establishment of the annual system performance. For illustration all hydraulic schemes are presented in (5.19). In addition, what is not shown, the seven systems have seven different control strategies and settings, for the collector loop, the space heating loop(s) as well as the auxiliary heater(s). For example in all seven systems the collector loop control strategy can be changed to matched flow (i.e. the mass flow is adjusted to allow the return temperature to match the return location in the storage tank). The results are shown in (5.20). The analysis of Combi systems is thus significantly more complex than for SDHW systems. As mentioned before Combi systems have additional return flows into

the tank from discharge loop(s) (i.e. the space heating loop). In addition is it also more difficult to manage the temperature of the return flows and the mass flow (another control strategy is the stratified return see(5.21)). With increasing collector area (for the Combi system we have a minimum of 12m^2) the mass flow is usually also larger causing more stratification disturbances. The temperature (and mass flow) of the space heating loop depends on the space heating devices used (radiator heating or floor heating), the temperature settings in this loop and the way these loops are controlled (i.e. mass-flow and temperature level and temperature drop). Combi systems are also available in more (hydraulic) variations than SDHW systems, causing the issue of which system configuration is considered representative.

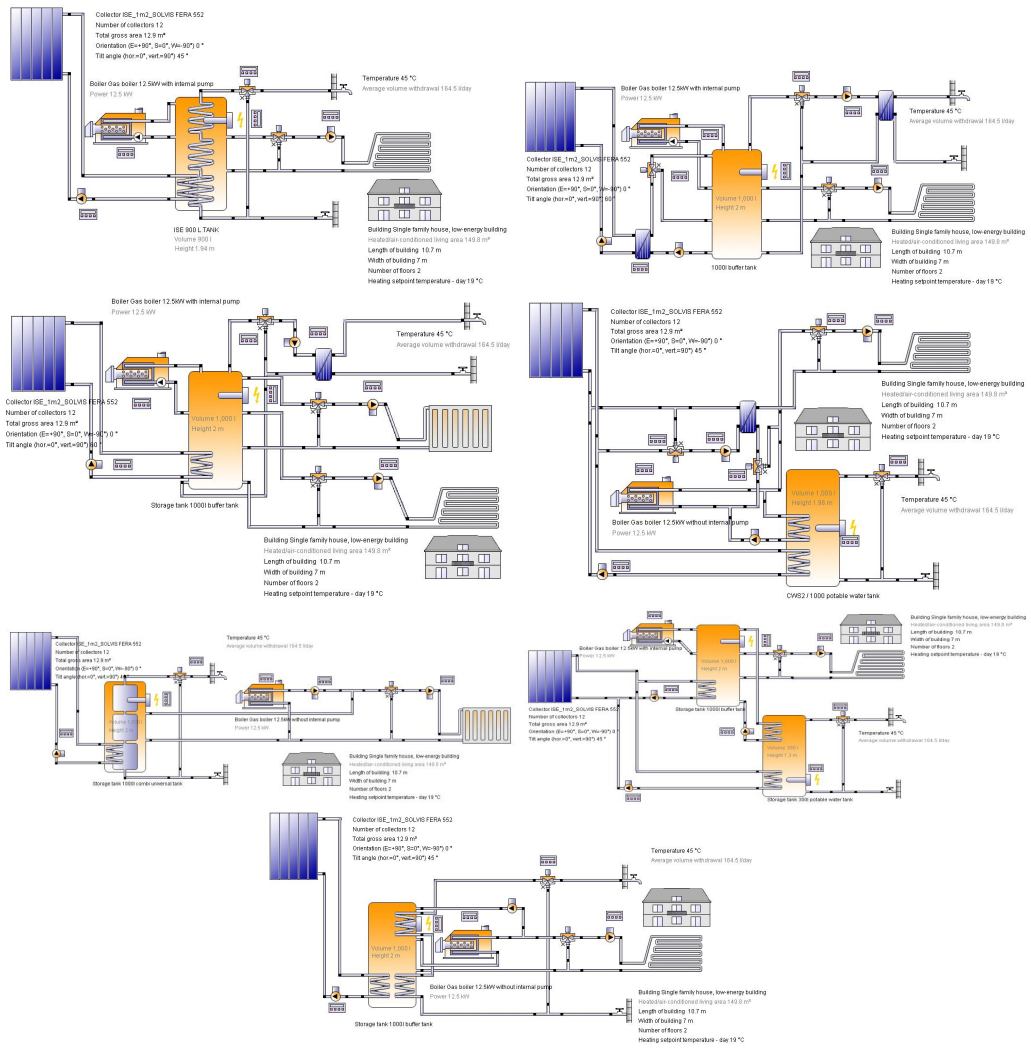


Figure 5.19: Seven Hydraulic schemes of standard Combi system configurations. From top to bottom: tank in tank, fresh water station, 2 heating loops, direct space heating, tank in tank (electric, gas boiler), 2 tanks direct DHW and modular heat generator

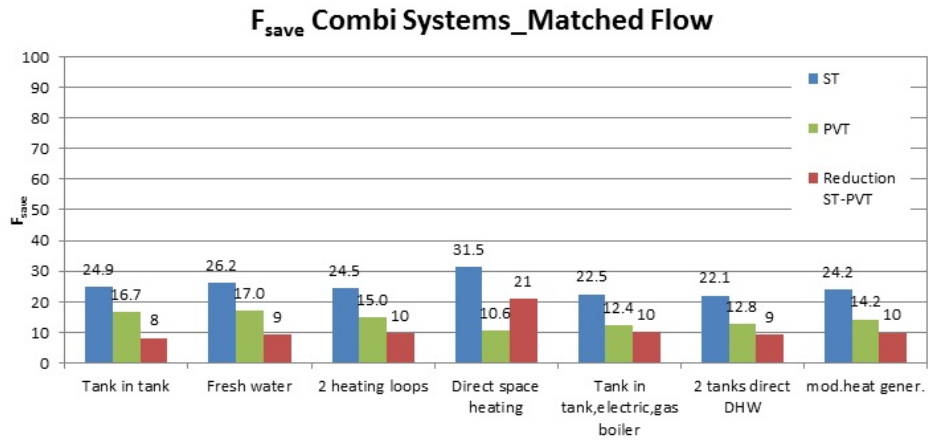


Figure 5.20: F_{save} CombySystem LowEnergy MatchedFlow

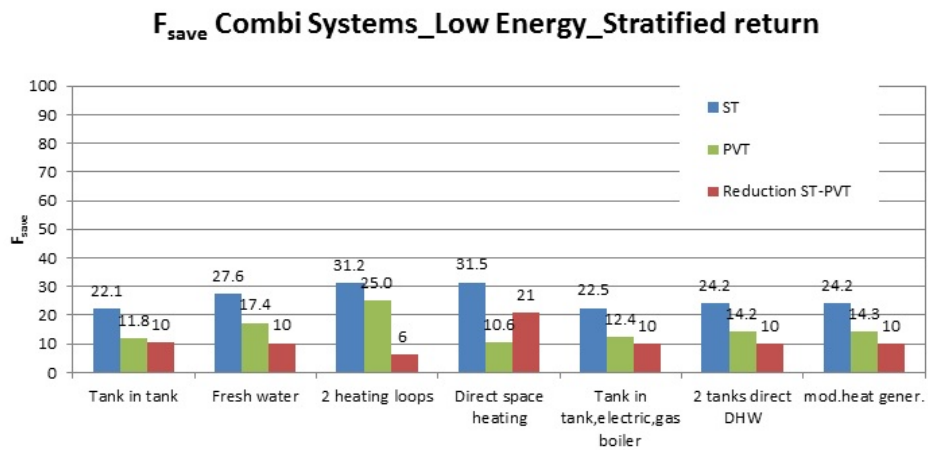


Figure 5.21: F_{save} CombySystem LowEnergy Stratifiedreturn

5.2.3 Large solar fraction system (SF-House)

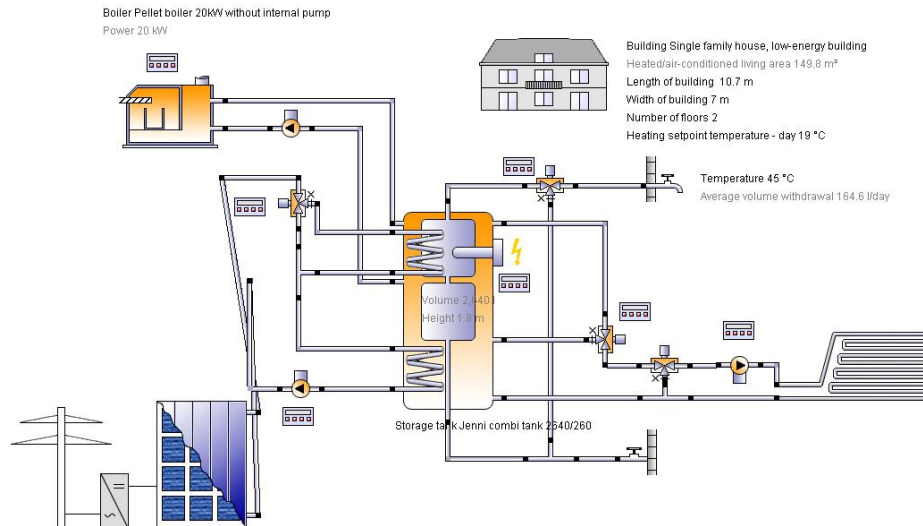


Figure 5.22: Scheme PVT COMBI LARGER F_{save}

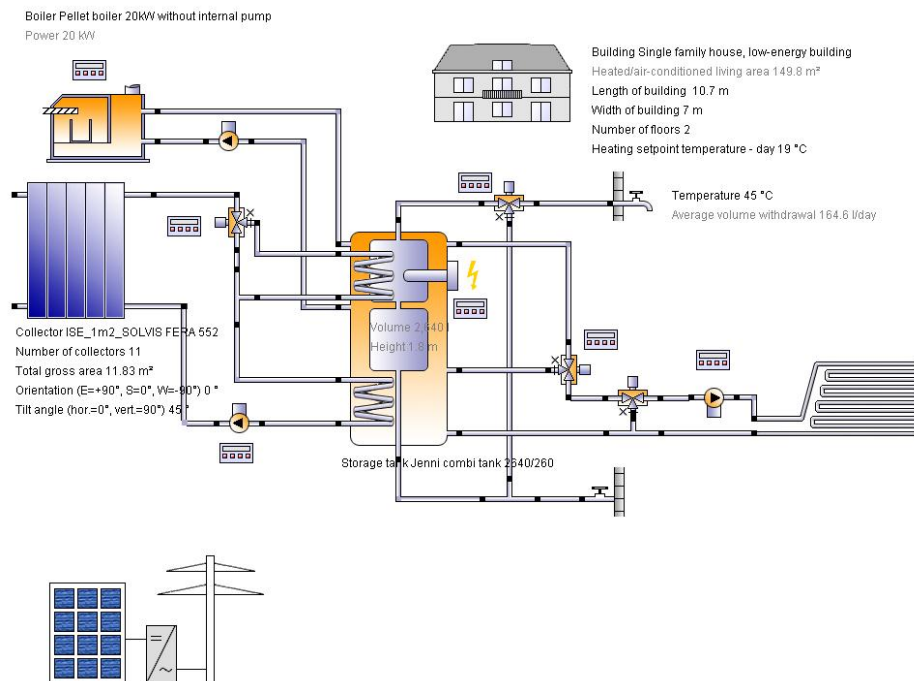
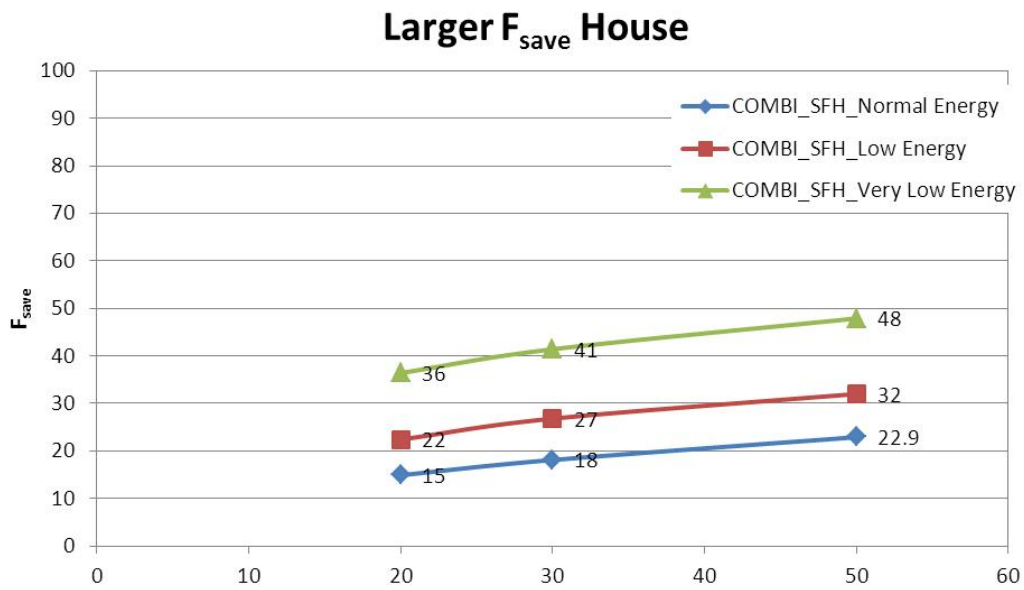


Figure 5.23: Scheme ST+PV COMBI LARGER F_{save}



same as this:

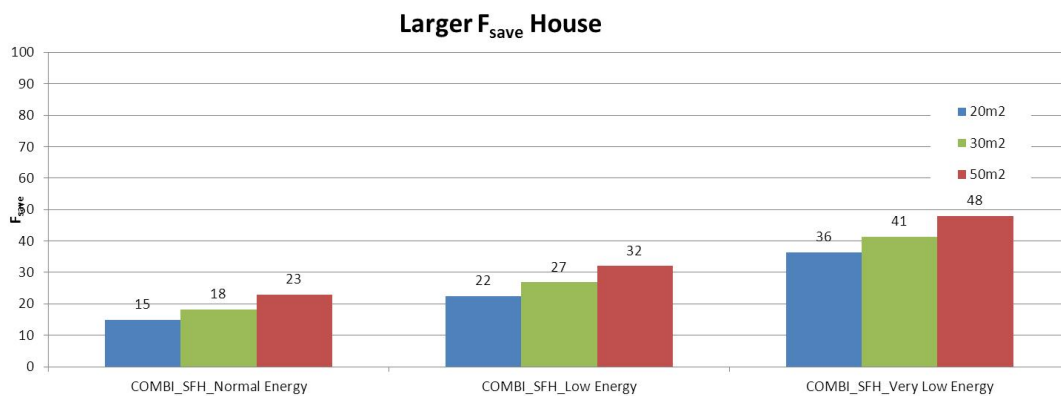


Figure 5.24: Larger F_{save} Table results

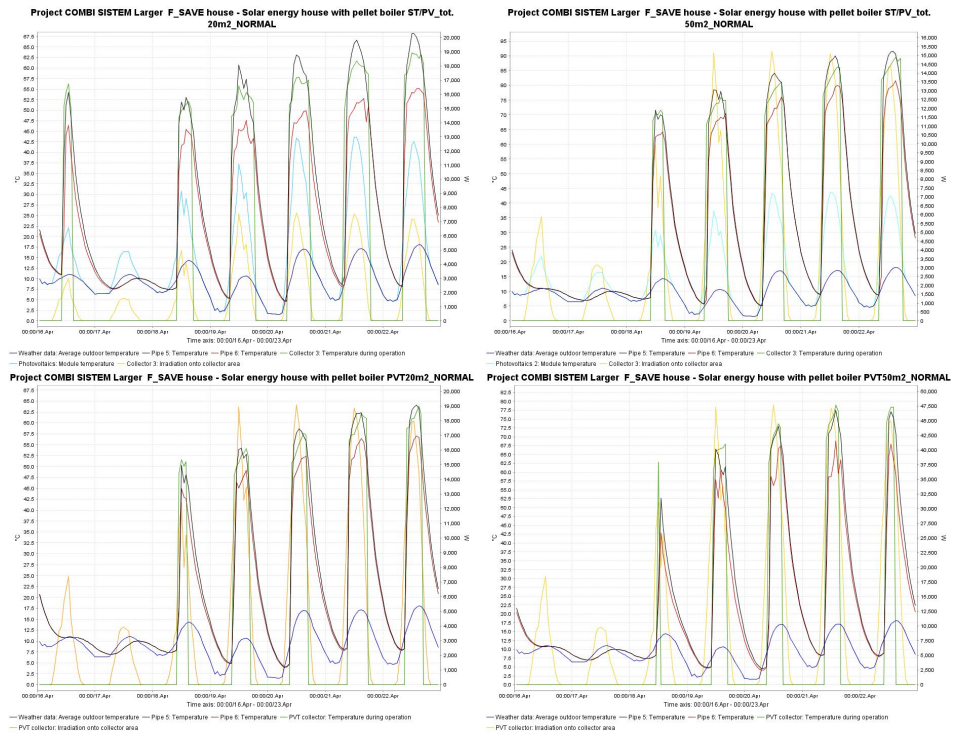


Figure 5.25: Tgraph Larger F_{save} area (Average outdoor temperature, T_{incol} , T_{outcol} , $T_{coll-ope}$, Irradiation onto collector area)

Looking at the Tgraphs we can see for 50m² area the lower value of collector operating temperature as compared to the solar thermal one due to different insulation but, to the contrary of previous simulations, the change in collectors operating time is evident. Solar thermal device starts working earlier and finishes later and this is why is much more efficient for hot water and space heating demand.

5.2.4 Solar and Heat Pump (Solar+HP)

The aim of this chapter is to assess Combi systems using a heat pump as auxiliary heater and PVT solar collectors. In scope are the options of a gas fired or heat pump auxiliary heater, in combination with ST, PVT and PV collectors. All systems have 12m² collectors area except where mentioned only. The results are displayed in 5.26. The evaluation criteria include $F_{save\ thermal}$ (solar thermal savings in end-use energy), $F_{save\ primary}$ (primary energy saved, which includes primary to end-use conversion losses and PV electricity generation) and Primary energy balance (which includes the electricity generated). Only PV and PVT systems can offset some primary energy demand with elec-

tricity generated (this is the difference between primary energy demand and primary energy balance). Energy conversion factors used:

- Gas fired boiler efficiency: 0.885%
- Electricity efficiency: 0.4%

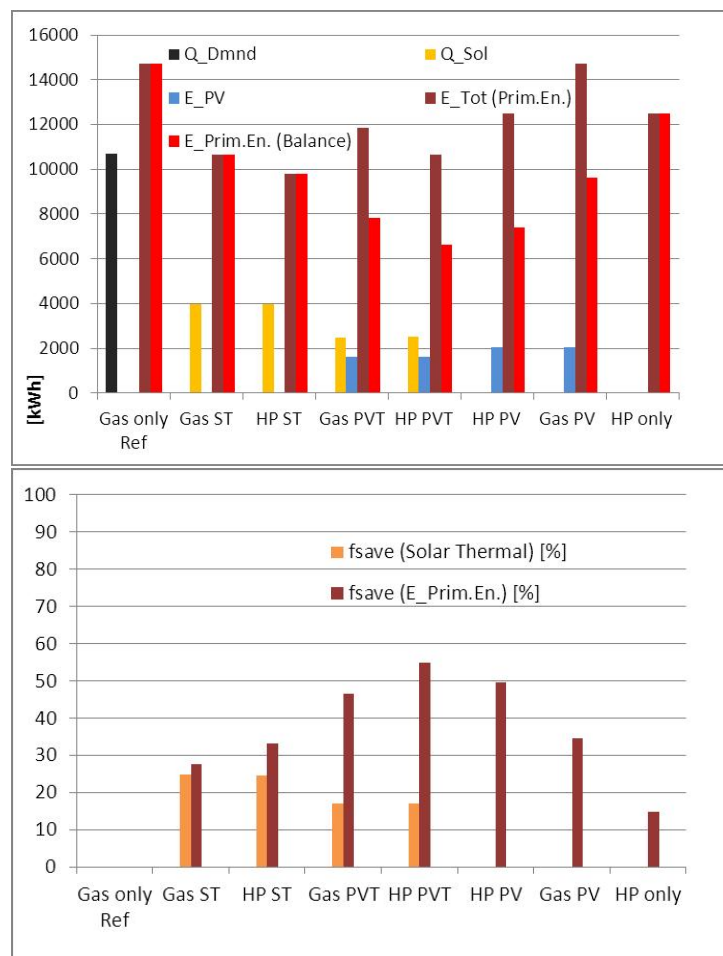


Figure 5.26: Results of (3) Gas fired, (4) heat pump and (5) solar (ST, PVT and PV) system configurations compared based on energy flows and energy savings.

The reference system in any of the comparisons is always the system with gas (only) fired boiler. The following can be observed and concluded from 5.26: The primary energy used by the HP (only) system is (15%) less than that of the gas fired (only) system. The HP system is thus more efficient

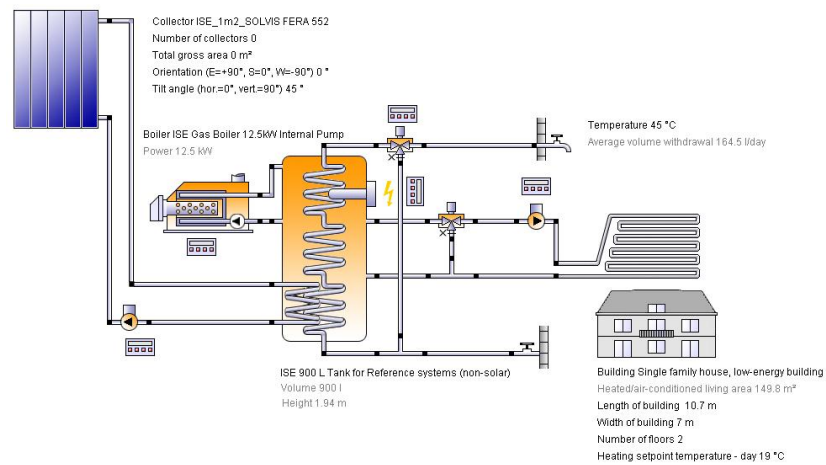


Figure 5.27: Gas (only) fired boiler system (reference for all other systems regarding savings calculations). Note that in this system (gas only) the collector area is zero.

than the gas fired system in terms of primary energy use. But more primary energy is saved with any of the solar systems than that of the HP (only) system. The HP ST system has the lowest primary energy demand, but not the lowest primary energy balance. Although the $F_{save\ thermal}$ (primary energy needed) for the PVT systems is worse than that of the ST systems, the primary energy balance (and thus the $F_{save\ primary}$ is much better. In fact, the combination HP PVT has the best primary energy balance, and the HP PV combination comes in as a good second. Below two system configurations representative for the configurations used (5.27-5.28).

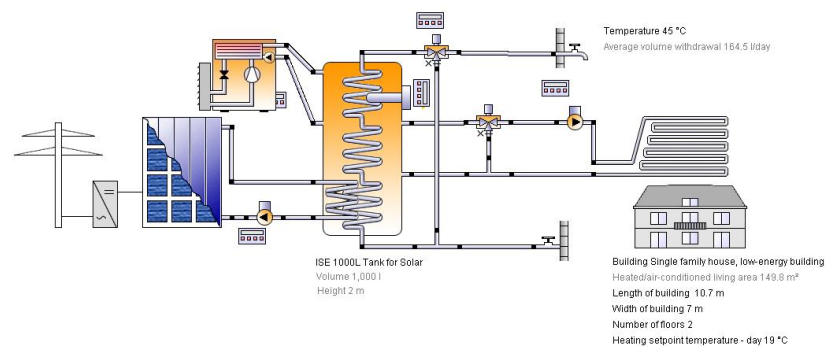


Figure 5.28: HP and PVT combination system (with the best primary energy saving of all systems).

Suggestion for further inclusion of simulation:

1. Above only the low energy house ($50kWh/m^2/y$) is used: could include normal house ($100kWh/m^2/y$, not much use), better is to include the very low energy house (Passive, $25kWh/m^2/y$).
2. Still to show the temporal (time) mismatch in electricity supply (mainly summer) and demand (winter) (monthly overview of the above values, probably only for the HP PVT system).

5.2.5 Solar Heat pump (integrated)

Further future investigations will regard Combi systems with combined operation of PVT solar collectors and a heat pump in the collector loop. Systems will be changed step by step from the standard combi system towards the best system with integrated HP and borehole. For systems with a heat pump, solar collectors and a borehole the collector and borehole are permanently in series (the outlet of the collector always passes through the borehole before going to the heat pump). For borehole regeneration the heat pump can be bypassed. A more complex solution consists of a collector loop with separate bypasses for the following optional components in the loop: store heat exchangers, borehole and heat pump.

Chapter 6

Conclusions

In this thesis a thermophotovoltaic hybrid panel for the combined production of heat and electricity has been analyzed and studied from different points of view: numerical absorber profile optimization by means of genetic algorithms, experimental efficiency evaluation, collectors modeling and finally definition of system boundaries. The following summaries present the most important results obtained from each chapter.

In Chapter II using a multi-objective genetic algorithm numerical analysis, the aim has been the optimization of the internal channel geometry of an industrial commercial heat sink in order principally to maximize the equivalent Nusselt number and the compared effectiveness related to the standard profile. Besides the Re_{max} limits, the condition of constrained finned plate volume has been taken into account imposing the average thickness σ_s . After fixing the order of the polynomial function which describes the fin profile (from 1st to 4th order) a starting profile has been chosen as a prototype. It is evident from results the thermal efficiency improving of our heat sink due to channel profile modifications from 2nd to 4th order. But for a realistic analysis you have, anyway, to reach and choose for the profile an optimum compromise between thermal efficiency and constraints as fixed volume, hydraulic resistance and profiles local convective thermal exchange in order to obtain the best solution (little less performing but technically and economically feasible).

In Chapter III the PVT system has been studied experimentally outdoor to assess the increase in performance for a particular Italian north-east location (Forlì) as part of a closed loop single phase water CDU (coolant dis-

tribution unit) in laminar forced convection. The daily tests, carried out from early morning in summer to late afternoon in autumn regarding two different measuring years(2011 -2012), have been done in comparison with photovoltaic and solar thermal systems. The efficiency values have been measured to compare ST, PVT and PV outputs under the same outdoor operating conditions. It is noticeable that the average annual electric efficiency gain due to cell cooling is rather high (15-20%). Results show that hot cell temperature reaches 60°C in the hottest hours of a summer day, very far from standard project ambient temperature (25°C). Also in middle seasons, despite a lower thermal exchange, cells temperatures are always higher than 25°C thus a positive efficiency gain is always obtained for the specific operating values analyzed. From the thermal point of view the average annual efficiency is 10 ÷ 15% less than the solar thermal collector. Besides PV cell electric conversion, the most important difference between solar thermal and PVT thermal efficiency curves regards absorber spectral properties. While the absorber of a thermal collector shows high absorption in the solar spectrum range and low emissivity in the infra-red spectrum, the PV cell surface features present lower absorbance and higher emissivity. Moreover PVT has an additional thermal resistance between absorber and cells due to the additional layer of thermal paste (aluminium oxide-filled double component epoxy in the present case) used to connect the module and the absorber. These results show that the principal aim has to be the optimization of all PVT absorbing package materials(PV cells, collector geometry, insulation, coatings)trying to reach the physical and technical limits of this technology making it economically comparable at last with separated productions.

Chapter IV presents a part of PVT research work carried on at Fraunhofer Solar Institute. The research has regarded first of all the creation of new PVT and solar thermal equation based models built thanks to Dymola software that uses Modelica language. These models have been compared with experimentally validated ones previously developed at Fraunhofer through different Excel sheets. Using Excel sheets there are a lot of possibilities to make a model strong detailed with all input cells connected one by one with own formulas and to create graphs from it. But from the solving mathematical point of view there are some limitations(external solver, limited model flexibility and lack of a user-friendly interface). Differently, at the top level of the new PVT and solar thermal models I've defined the parameters and all the other fixed values that do not change and are used in the model. The strongest possibility and feature of this model is first of all the flexibility of system modifications and subsequent collector test simulations. We are free

to create our own model libraries or modify the ready-made model libraries to better match simulation needs. Efficiency curve results from the two models compared differ one from the other less than $\pm 5\%$.

The second part of my Fraunhofer research has been devoted to identify possible approaches for PVT collectors and systems. The analysis here focusses on the thermal yield of solar thermal systems operating with flat plate PVT collectors compared to systems operating with conventional flat plate solar thermal collectors. The performance of solar systems is usually judged in terms of energy (F_{save}) or cost savings in comparison to a similar conventional non-solar heating system (natural gas, oil or electricity). The difference in thermal performance depends mainly on the following single, controllable system factor:

- The temperature of the fluid flowing into the collector inlet (T_{inlet}).

A higher inlet temperature leads to a lower (instantaneous) thermal efficiency of the collector. A lower instantaneous efficiency at the operating point (dT/G or dT) leads to a lower energy yield by the collector.

From SDHW (solar domestic hot water) Polysun simulations results it can be concluded that a change from $4m^2$ to $6m^2$ collector area does not increase the yield proportionally, but only 10-11% for covered collectors and very little (1-2%) for uncovered PVT collectors. The thermal yield of the uncovered PVT collectors can be ruled insufficient for use of these collectors in auxiliary heated SDHW systems. The use of the solar pre-heat system configuration (with continuous flow heater before the tap) is still most beneficial for the uncovered PVT collectors, but the yield is still doubtfully low. The covered PVT collectors also achieve a much lower yield than the ST collectors. A lower auxiliary heater set point, e.g. 52.5°C instead of 62.5°C , is clearly beneficial for SDHW systems, even more for PVT collectors than ST collectors. The continuous flow heater systems provides the best yield increase for the PVT collectors and is the preferred option for SDHW systems with PVT collectors. Further simulations conclude also that an F_{save} equal to that of 4 or $6m^2$ of ST collectors (63.0% resp. 72.5%) cannot be achieved with the PVT uncovered collector. A comparison between the auxiliary heated and pre-heat system graphs also shows that the optimum for the pre-heat system is reached at larger collector areas than for the (52.5°C) auxiliary heated system. Using a continuous flow heater in a pre-heat SDHW system combination is more beneficial for the PVT collector (18% and 26% reduction

in collector area) than the ST collector (7% reduction). By improving the solar heating system (using a solar pre-heat system instead of an auxiliary heater with set point at 62.5°C) the improved PVT collector can achieve the $60\%F_{save}$ with only a 13% larger collector area (5.6m^2 instead of 4.9m^2). We evaluate also which is the influence of the auxiliary store heating on the collector and store temperatures: the collector inlet temperature, collector outlet temperature and collector operating temperature are all higher for the auxiliary (store) heated system, thus the collector operating efficiency in this system is lower. In addition it can be seen that the operating times is generally narrower for the auxiliary heated system compared to the pre-heat one. A comparison of the pre-heat systems graphs resp. with 4 and 6 m^2 of uncovered PVT collectors shows the slightly higher temperatures (collector inlet temperature, collector outlet temperature and collector operating temperature) and (sometimes) slightly shorter operating times for the system with larger collector area. Although the available solar radiation is larger for the system with larger collector area, the much reduced collector efficiency due to slightly higher operating temperatures compensates this benefit

Concerning the COMBI system analysis, we see that the annual yield of the system with PVT collectors is $1/3$ (for 52.5°C) to almost $1/2$ (for 62.5°C) less than that of the one with solar thermal collectors. Through reducing the auxiliary heating temperature and lowering the heating demand the difference between the energy yield from the ST and PVT collectors, can be reduced from 41-47% to 30-35%. The largest differences are between systems using ST and PVT collectors in the normal energy house with high auxiliary heating setting temperature and also between the systems with different auxiliary heating temperatures for the very low energy houses using PVT collectors. The (large) difference in yield between the Combi systems using PVT collectors with auxiliary temperature setting 62.5°C (top, $F_{save} = 24\%$) and 52.5°C (bottom, $F_{save} = 29\%$) is caused by differences in collector operating efficiency due to different collector operating temperatures of $2.5 - 5^{\circ}\text{C}$ higher, although the operating times are similar. From this it can be also concluded that for Combi system:

- A reduction in the auxiliary temperature setting is beneficial for all systems and in particular for those with PVT collectors because it leads to higher operating efficiencies.
- A larger imbalance between energy supply and demand (quantitatively and temporal) is only slightly more detrimental for the system with PVT collector than that with solar thermal only collector.

The results of 7 different (standard) Combi systems shows that the yield varies strongly per system, from $F_{save} = 22\%$ to 29% for systems with ST collectors and from 11% to 20% for systems with PVT collectors. The size of the variability is principally due to different control strategies and settings (es. matched flow and stratified return) for the collector loop, the space heating loop(s) as well as the auxiliary heater(s). With increasing collector area (for the Combi system a minimum of 12m^2) the mass flow is usually also larger causing more stratification disturbances. The analysis of Combi systems is thus significantly more complex than for SDHW systems, causing also the issue of which of the various different hydraulic configuration is considered representative.

Looking at the Tgraphs of large solar fraction house, we can see for 50m^2 area the lower value of PVT collector operating temperature respect of solar thermal one due to different insulation but it is evident the difference on collectors operating time (solar thermal device starts working early and finishes lately).

The section Solar and Heat Pump has the aim to assess Combi systems using a heat pump as auxiliary heater and PVT solar collectors. In scope are the options of a gas fired or heat pump auxiliary heater, in combination with ST, PVT and PV collectors. All systems have 12m^2 of collectors. The evaluation criteria include: $F_{save\,thermal}$ (solar thermal savings in end-use energy), $F_{save\,prim}$ (primary energy saved, which includes primary to end-use conversion losses and PV electricity generation) and Primary energy balance (which includes the electricity generated). Only PV and PVT systems can offset some primary energy demand with electricity generated (this is the difference between primary energy demand and primary energy balance). The reference system in any of the comparisons is always the system with gas (only) fired boiler. From the results the following conclusions :

- The primary energy used by the HP (only) system is (15%) less than that of the gas fired (only) system.
- The HP system is thus more efficient than the gas fired system in terms of primary energy use. But more primary energy is saved with any of the solar systems than that of the HP (only) system.
- The HP ST system has the lowest primary energy demand, but not the lowest primary energy balance.

This detailed PVT analysis, following a multi-scale approach, starts from single PVT devices optimization trying at last to find boundary solutions for PVT glazed collector as a whole in a system . The results show that a lot of research has already been made and must be continued to improve PVT panel. Possible future investigations include for example PV silicon cell properties(texturing and metallization improvements), new PV module lamination methods and development of new packages(channel geometries, insulation material, glass cover). It is obvious infact from previous published results and this thesis that PVT panel could be very performing due to high density energy power and its good system integration. Once some technical problems are fixed so as to make the system comparable not only from the efficiency point of view but also economically with both the separate technologies, this PVT panel could be really competitive in itself and principally in aggregate with heat pumps or borehole heat exchangers in solar assisted integrated systems.

Appendix A

Fluid and Materials: Temperature dependance

Concerning our equation based models we have taken fluid and materials properties temperature independent within the range of operating temperatures, but in order to calculate in detail the convective heat transfer between the absorber plate and the glass cover of a solar thermal and PVT collector the temperature dependance of fluid and materials properties must be known.

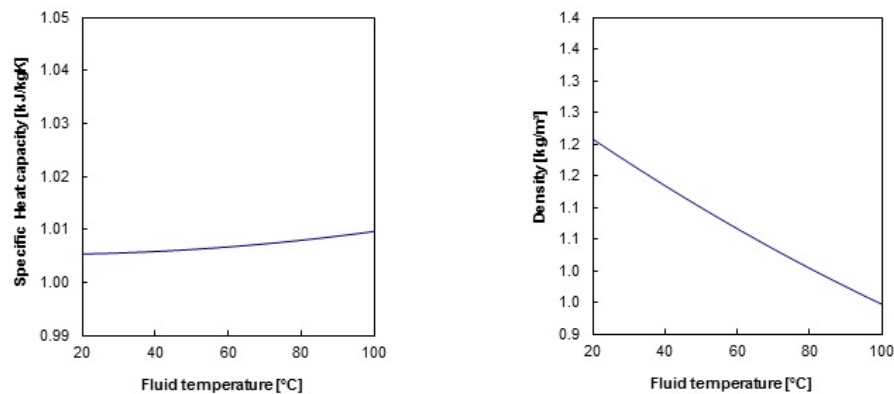


Figure A.1: Air properties (source:www.engineeringtoolbox.com)

(A.1-A.2) presents the variation of density, kinematic viscosity, specific heat capacity and thermal conductivity of air in the range of temperature corresponding to solar thermal and PVT operation. Also to calculate the forced convection in the pipe of the absorber of a thermal collector, the thermal dependancy of water properties must be known. (A.3-A.4) presents

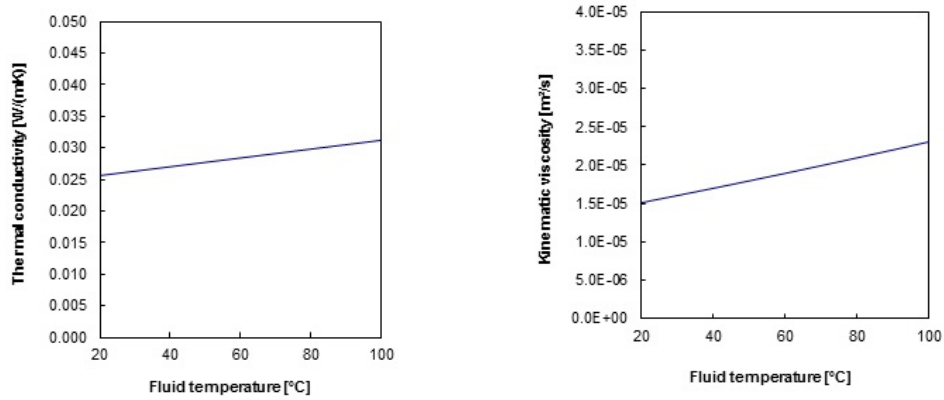


Figure A.2: Air properties(source:www.engineeringtoolbox.com)

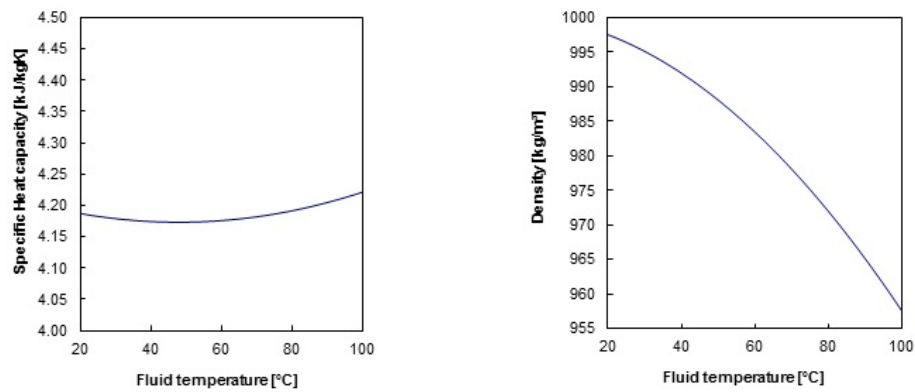


Figure A.3: Water properties(source:www.engineeringtoolbox.com)

the variation of density, cinematic viscosity, specific heat capacity and thermal conductivity of water in the range of temperature corresponding to collectors uses.

In addition of the change in terms of emissivity related to an increase of the absorber temperature, the change in terms of thermal conductivity of the thermal insulating material located around and below the absorber must be known. A.5 presents the variation of the thermal conductivity of the insulating material used for our mobile experimental structure in the range of operating temperature for solar thermal and PVT.

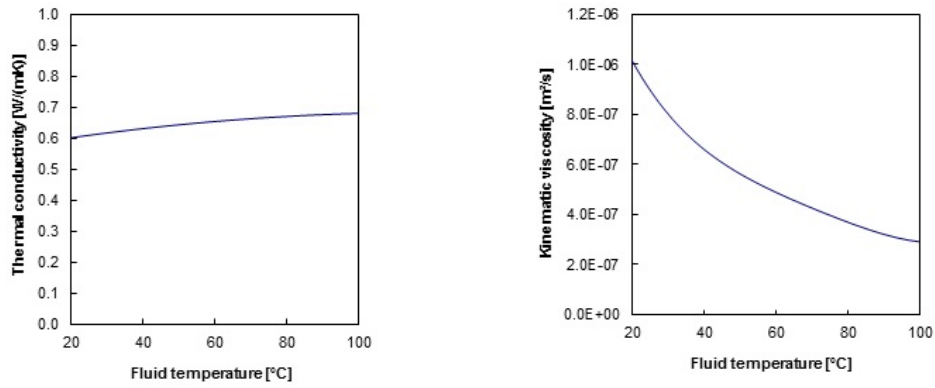


Figure A.4: Water properties(source:www.engineeringtoolbox.com)

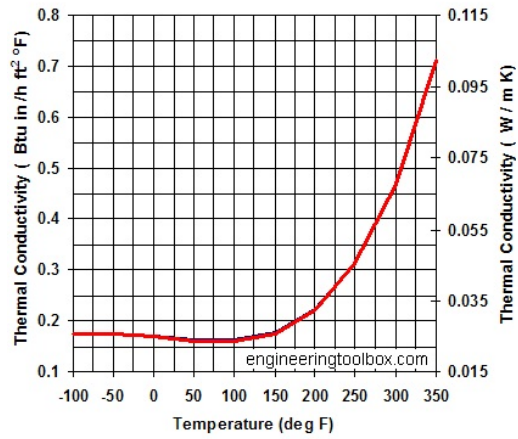


Figure A.5: Polyurethane foam(source:www.engineeringtoolbox.com)

Acknowledgements

First of all I'd like to thank my supervisor Prof. Giampietro Fabbri for his scientific and guidance support during my three years PhD research about thermophotovoltaic panels. During these three years I've been able to analyze different aspects regarding thermophotovoltaic panels from the numerical and experimental point of view discovering possibilities and limits of this technology.

I thank also Mr. Fortuin and Mr. Stryi-Hipp together with I've collaborated during my exchange Marcopolo programme at Fraunhofer ISE (Freiburg) in order to complete my analysis on different PVT topics. I've exchanged experiences in a very open-minded structure and I hope to work again with them on different projects in future.

I'd like also to give my thanks to people who have worked with me during these years and they have helped and supported me with some aspects of the research (Paolo, Riccardo and Marco).

Particularly I'd like to thank Andrea that was the one that mostly has beared me during working time.

And finally and foremost my family (my parents Fausto and Licia and my sister Chiara) for all they have always done for me, all my friends and the other people who have really supported me when I needed.

Thanks to all
Matteo

Bibliography

- [1] Zondag, H. A., “Flat-plate PV-Thermal collectors and systems:A review”, *Renewable and Sustainable Energy Reviews*, **12**:891-959(2008).
- [2] Boer ,K.W., “A combined solar thermal and electrical House system”, *Proceedings of the International Congress on Sun in the Service of Mankind*,Paris,(1973).
- [3] Boer ,K.W., “Solar retrofitting of existing residence with almost zero-delta Te system”, *International Conference New Dehli*,(1978).
- [4] Tiwari, A.,Sodha, M.S., “Performance evaluation of hybrid PVT water/air heating system: A parametric study”, *Renewable Energy*, **31**:2460-2474(2006).
- [5] Zondag, H. A., de Vries, D. W., Van Helden ,W. G. J., and Van Steenhoven, A. A., “Thermal and electrical yield of a hybrid-panel”, *Proceedings of ISES Conference Jerusalem* ,(1999).
- [6] Chow, T.T., “Energy and exergy analysis of photovoltaic-thermal collector with and without glass cover” *Applied Energy*, **86(3)**:310-316(2009).
- [7] Zondag, H. A., de Vries, D. W., Van Helden ,W. G. J., Van Zolengen,R. J. C. and Van Steenhoven, A. A., “The yield of different combined PV-thermal collector designs” , *Solar Energy*, **74**:253-269(2003).
- [8] Cristofari ,C.,Notton ,G.,Canaletti ,J.L., “Thermal behaviour of a copolymer PV/Th solar system in low flow rate conditions”, *Solar Energy*, **83(8)**:1123-1138(2009).
- [9] Duffie,J.A.,Beckman ,W.A., “Solar Engineering of Thermal Processes”, *John Wiley and Sons Inc*, New York,1991.
- [10] Kalogirou,S.A.,Tripanagnostopoulos ,Y., “Hybrid PV/T solar systems for domestic hot water and electricity production”, *Energy Conversion and Management*, **47(18-19)**:3368-3382(2006).

- [11] Huang,B.J.,Lin,T.H.,Hung,W.C., “Performance evaluation of solar photovoltaic/thermal systems”, *Solar Energy*, **70(5)**:443-448(2001).
- [12] Fujisawa ,T.,Tani,T., “Annual exergy evaluation on photovoltaic-thermal hybrid collector”, *Solar Energy Materials and Solar Cells*, **47**:135-148(1997).
- [13] Charalambous, P.G.,Maidment ,G.G.,Kalogirou ,S.A.,Yiakoumetti ,K., “Photovoltaic thermal(PV/T)collectors:a review”, *Applied Thermal Engineering*, **27(2-3)**:275-286(2007).
- [14] Ibrahim,A.,Othman.,M.Y.,Ruslan,M.H.,Mat,S.,Sopian,K., “Recent advances in flat plate photovoltaic thermal(PV/T)solar thermal collectors”, *Renewable and Sustainable Energy Reviews*, **15(1)**:352-365(2011).
- [15] Dumont, “Water-cooled electronics”, *Nuclear Instruments and Methods in Physics* , **A440**:213-223(2000).
- [16] Santbergen,R.,Rindt.,C.C.M.,Zondag,H.A.,van Zolingen,R.J.Ch., “Detailed analysis of the energy yield of systems with covered sheet-and-tube PVT collectors”, *Solar Energy*, **84**:867-878(2010).
- [17] Dupeyrat ,P.,Menezo ,C.,Fortuin,S., “Study of the thermal and electrical performances of PVT solar hot water systems”, *Energy Buildings*, (2012).
- [18] Dupeyrat,P.,Menezo.,C.,Rommel,M.,Henning,H.M., “Efficient single glazed flat plate photovoltaic thermal hybrid collector for domestic hot water system ”, *Renewable and Sustainable Energy Reviews*, **15(1)**:352-365(2011).
- [19] Fabbri G., “Optimum performances of longitudinal convective fins with symmetrical and asymmetrical profiles”, *International Journal of Heat and Fluid Flow*, **20**:634-641(1999).
- [20] Copiello ,D.,Fabbri, G., “Multi-objective genetic optimization of the heat transfer from longitudinal wavy fins”, *International Journal of Heat and Mass transfer* , **52**:1167-1176(2009).
- [21] Fabbri ,G., “Heat transfer optimization in internally finned tubes under laminar flow conditions”, *International Journal of Heat and Mass Transfer* , **41(10)**:1243-1253(1998).

- [22] Fabbri ,G.,Greppi ,M,Lorenzini ,M., “Optimization with Genetic Algorithm of PVT System Global Efficiency”, *Journal of Energy and Power Engineering*, **6(7)**:(2012).
- [23] *ISO Standard 9806-1*, “Test methods for solar collectors.Part 1: Thermal performance of Liquid heating collectors”, *ISO Switzerland*,(1994).
- [24] Smith C.,Weiss A., “Design application of the Hottel-Whillier-Bliss equation”, *Solar Energy*, **19**:109-113(1977).
- [25] Florschuetz ,L.W., “Extension of the Hottel-Whillier model to the analysis of combined photovoltaic/thermal flat plate collectors”, *Solar Energy*, **22(4)**:361-366(1979).
- [26] Bergene ,T.,Lovvik ,O.M., “Model calculations on a flat plate solar heat collector with integrated solar cells”, *Solar Energy*, **55(6)**:453-462(1995).
- [27] Matuska ,T.,Zmrhal ,V., “A mathematical model and design tool KOLEKTOR 2.2 reference handbook.Czech technical university of Prague”, (2009).
- [28] Vokas ,G.,Christandonis ,N.,Skittides,F., “Hybrid photovoltaic-thermal systems for domestic heating and cooling-A theoretical approach”, *Solar Energy*, **80**:607-615(2006).
- [29] Boddaert ,S.,Cacavelli ,C.,Menezo, C.,Morlot, R., “Hybrid PVT panel optimisation using a FEMLAB/MATLAB/SIMULINK approach”, *Proceeding of First International Conference on Environment and Identities in the Mediterranean ISEIM*, Corte-Ajaccio(2006).
- [30] Cristofari,C.,Notton.,G.,Poggi,Louche,A., “Influence of the flow rate and the tank stratification degree on the performances of a solar flat plate collector”, *International Journal of Thermal Sciences*, **42**:455-469(2003).
- [31] Glembin J., Rockendorf G., “Simulation and evaluation of stratified discharging and charging devices in combined solar thermal system”, *Solar Energy*, **86(1)**:407-420(2012).
- [32] Greppi M., Fortuin S., “Joint work finalized by M.Greppi and S.Fortuin during Fraunhofer ISE Marcopolo PhD exchange”, *2012*.

- [33] Bakker ,M.,Zondag ,H.A., “Performance and costs of a roof sized PVT array combined with a ground coupled heat pump”, *Solar Energy*, **78(2)**:331-339(2005).